Articles

Interactions of the HIV-1 Tat and RAP74 Proteins with the RNA Polymerase II CTD Phosphatase FCP1†

Karen L. Abbott,[‡,¶] Jacques Archambault,[§,¶] Hua Xiao,[||,¶] Bao D. Nguyen,[‡,¶] Robert G. Roeder,[||] Jack Greenblatt,[§] James G. Omichinski,*[,‡,⊥,¶] and Pascale Legault*[,‡,¶]

Department of Biochemistry and Molecular Biology and Department of Chemistry, University of Georgia, Athens, Georgia, 30602, Banting and Best Department of Medical Research and Department of Medical Genetics and Microbiology, University of Toronto, 112 College Street, Toronto, Ontario, Canada M5G 1L6, and Laboratory of Biochemistry and Molecular Biology, Rockefeller University, New York, New York 10021

Received September 22, 2004; Revised Manuscript Received November 18, 2004

ABSTRACT: FCP1, a phosphatase specific for the carboxyl-terminal domain of the largest subunit of RNA polymerase II, is regulated by the HIV-1 Tat protein, CK2, TFIIB, and the large subunit of TFIIF (RAP74). We have characterized the interactions of Tat and RAP74 with the BRCT-containing central domain of FCP1 ($FCP1_{562-738}$). We demonstrated that FCP1 is required for Tat-mediated transactivation in vitro and that amino acids 562−685 of FCP1 are necessary for Tat interaction in yeast two-hybrid studies. From sequence alignments, we identified a conserved acidic/hydrophobic region in FCP1 adjacent to its highly conserved BRCT domain. In vitro binding studies with purified proteins indicate that HIV-1 Tat interacts with both the acidic/hydrophobic region and the BRCT domain of FCP1, whereas $RAP74_{436-517}$ interacts solely with a portion of the acidic/hydrophobic region containing a conserved LXXLL-like motif. HIV-1 Tat inhibits the binding of $RAP74_{436-517}$ to FCP1. In a companion paper (K. Abbott et al. (2005) Enhanced Binding of RNAPII CTD Phosphatase FCP1 to RAP74 Following CK2 Phosphorylation, *Biochemistry 44*, 2732−2745, we identified a novel CK2 site adjacent to this conserved LXXLL-like motif. Phosphorylation of $FCP1_{562-619}$ by CK2 at this site increases binding to $RAP74_{436-517}$, but this phosphorylation is inhibited by Tat. Our results provide insights into the mechanisms by which Tat inhibits the FCP1 CTD phosphatase activity and by which FCP1 mediates transcriptional activation by Tat. In addition to increasing our understanding of the role of HIV-1 Tat in transcriptional regulation, this study defines a clear role for regions adjacent to the BRCT domain in promoting important protein−protein interactions.

Transcription by RNA polymerase II (RNAPII) is a complex process regulated in part by the phosphorylation of the carboxyl-terminal domain (CTD) of the largest subunit of RNAPII (*1*, *2*). The RNAPII CTD contains several heptapeptide repeats that are phosphorylated during the transcription cycle (*3*). Transcription begins with the recruitment of the hypophosphorylated form of the polymerase (RNAPIIA). Following the assembly of the initiation complex, several kinases, such as cdk7 and cdk9, are recruited, allowing hyperphosphorylation of the CTD (*4*, *5*). The hyperphosphorylated form of the polymerase (RNAPIIO) is the form primarily found in elongating complexes (*1*, *6*). Upon completion of transcription, the CTD must be dephosphorylated before recycling of the polymerase can occur.

FCP1 is the only known phosphatase associated with RNAPII that specifically dephosphorylates the CTD of the largest subunit. FCP1 plays an important role in RNAPII

† This work was supported by the National Institutes of Health Grant RO1 GM60298-01 (to J.G.O. and P.L.) and by a grant from the Canadian Institutes of Health Research (to J.G.).

* Corresponding authors. Phone: 514-343-7326 (Legault) or 514-343-7341 (Omichinski). Fax: 514-343-2210. E-mail: pascale.legault@umontreal.ca or jg.omichinski@umontreal.ca.

‡ Department of Biochemistry and Molecular Biology, University of Georgia.

§ University of Toronto.

|| Rockefeller University.

⊥ Department of Chemistry, University of Georgia.

¶ Present addresses: K.A., Complex Carbohydrate Research Center, 315 Riverbend Rd., Athens, GA 30605; J.A., Institut de Recherches Cliniques de Montréal, 110 Avenue des Pins Ouest, Montréal, Québec, Canada H2W 1R7; H.X., Eppley Cancer Institute, University of Nebraska Medical Center, Omaha, NE 68198-7696; B.D.N., 164 Rowland Hall, University of California, Irvine, CA 92697-4675; J.G.O. and P.L., Département de Biochimie, Université de Montréal, C.P. 6128, Succursale Centre-Ville, Montréal, QC, Canada H3C 3J7.

[1] Abbreviations: RNAPII, RNA polymerase II; CTD, carboxyl-terminal domain; FCP1, TFIIF-associated CTD phosphatase; hFCP1, human FCP1; yFCP1, yeast FCP1; BRCT, Brca-1 carboxyl terminus; TFIIF, general transcription factor IIF; RAP74, largest subunit of the general transcription factor TFIIF; CK2, protein kinase CK2; GST, glutathione-S-transferase; His_6, hexahistidine; TFA, trifluoroacetic acid; AT, 3-aminotriazole; IPTG, isopropyl-β-D-thiogalactoside; GSH, glutathione; HSQC, heteronuclear single quantum coherence; HRP, horseradish peroxidase; Pfam, protein families database of alignments; BLAST, basic local alignment search tool.

10.1021/bi047957p CCC: $30.25 © 2005 American Chemical Society
Published on Web 02/05/2005

recycling, because it processively dephosphorylates the CTD of the largest subunit of RNAPII (*7*−*9*) at Ser^2 and Ser^5 (*10*−*13*). FCP1 can dephosphorylate arrested elongation complexes and therefore may also help modulate phosphorylation levels of the elongating polymerase (*9, 14*). FCP1 has also been shown to enhance elongation, and this function is independent of its phosphatase activity (*9, 15*). These findings that FCP1 functions in elongation complexes suggest that FCP1 may remain associated with RNAPII during elongation. However, although FCP1 can form a stable interaction with RNAPIIA (*8, 16, 17*), and ChIP experiments suggest that FCP1 remains associated with RNAPII during elongation (*11*), no stable association with RNAPIIO has been reported (*16*).

Three domains have been identified in FCP1 based on sequence similarity between human FCP1 (hFCP1) and yeast FCP1 (yFCP1) (*18*). The amino terminus contains the FCP homology region with the conserved ΨΨΨDXDX(T/V)ΨΨ motif (Ψ is a hydrophobic residue) characteristic of a family of small molecule phosphotransferases and phosphohydrolases (*19, 20*). Yeast studies revealed that mutation of the first aspartic acid of this motif abolishes catalytic activity (*12*), and strains carrying this mutation in FCP1 are not viable, indicating that the phosphatase activity of FCP1 is essential in yeast (*19*). Yeast studies have also revealed that the central domain of FCP1 is essential for cell viability and phosphatase activity (*12, 21*). The highly acidic carboxyl-terminal domain is dispensable both for activity and viability, however it is capable of activating transcription when tethered to a promoter by fusion to a heterologous DNA-binding domain (*21*).

The central domain of FCP1 contains a conserved Brca-1 carboxyl-terminal (BRCT) domain. The BRCT domain is an independently folded domain of ~95 amino acid residues that appears to be important for mediating protein−protein interactions. BRCT domains have been identified in one or multiple copies in over 450 proteins, which function in cell cycle regulation, DNA repair, recombination, chromatin remodeling and transcriptional activation (*22*−*28*). Several high-resolution structures of various BRCT domains have been determined either as single domains (*29*−*32*) or as tandem repeats (*31, 33*−*35*). The BRCT fold is characterized by a four-stranded parallel β-sheet surrounded by two or three α-helices. In tandem BRCT domains, the two domains pack together in a head-to-tail arrangement to form a stable compact structure (*31, 33, 35*). Recently, it was found that the BRCT domains of Brca1 and PTIP specifically recognize phosphorylated protein targets, defining a new role for the BRCT domain in cellular signaling (*36, 37*). Although the BRCT domain of FCP1 is essential for viability and phosphatase activity (*9, 12, 21, 38*), its direct involvement in protein−protein interactions is not well understood at this time.

Several proteins have been shown to influence the functions of FCP1 as a phosphatase and as a positive elongation factor. The largest subunit of the general transcription factor TFIIF (RAP74) has been shown to stimulate FCP1 phosphatase activity (*39*), whereas the general transcription factor TFIIB prevents this stimulation by TFIIF (*39*). The carboxyl-terminus of FCP1 directly interacts with the carboxyl-terminal domain of RAP74 (*8*) and the first cyclin repeat of TFIIB (*21*). The HIV-1 transcriptional activator protein Tat inhibits the dephosphorylation of the CTD by FCP1 (*40*). Also, both Tat and RAP74 interact with the central domain of FCP1 (*18, 21, 40*). Interestingly, Tat also interacts with the cellular kinase complex P-TEFb (cyclin T1 component) and has been shown to stimulate both Ser^2 and Ser^5 phosphorylation of the CTD (*41*). FCP1 contains multiple phosphorylation sites and recent studies have shown that phosphorylation regulates FCP1 activities (*42, 43*).

As part of our general interest in characterizing the molecular interactions that regulate the biological activity of FCP1, we recently described the first NMR structures of the carboxyl-terminal domain of RAP74 (cterRAP74) (*44*) and of a protein−protein complex between cterRAP74 and the carboxyl-terminal domain of FCP1 (*45*). In addition to providing a detailed view of this complex, our NMR studies confirmed the hypothesis that TFIIB and TFIIF share a common binding site on the carboxyl-terminal domain of FCP1 (*21, 44*). Here, we demonstrate that FCP1 is required for Tat-mediated transactivation in vitro and that the central domain of FCP1 is necessary for Tat interaction in yeast two-hybrid studies. We characterized the interactions of the BRCT-containing central domain of FCP1 ($FCP1_{562-738}$) with both the HIV-1 Tat protein and the carboxyl-terminal domain of RAP74. We also analyzed the effect of HIV-1 Tat on CK2 phosphorylation of purified $FCP1_{562-619}$ in vitro. We discuss the functional implications of the Tat/FCP1 interaction for the phosphatase activity of FCP1 and for Tat transcriptional activation.

EXPERIMENTAL PROCEDURES

Antibodies. The affinity-purified FCP1 polyclonal antibody was prepared as previously described (*8*). The HIV-1 Tat monoclonal antibody (15.1) and the Tat polyclonal antibody (705) used in this study were obtained through the NIH AIDS Research and Reference Reagent Program (*46, 47*). The RAP74 polyclonal antibody (C-18) and all secondary antibodies were purchased from Santa Cruz Biotechnologies (Santa Cruz, CA). The polyhistidine monoclonal antibody was purchased from Novagen (Madison, WI).

Plasmids. Plasmids used for yeast two-hybrid studies were constructed by inserting the indicated portion of human FCP1 and HIV-1 Tat in plasmids pAS-1 and pACTII, as described previously (*8*). Details of their construction will be provided upon request. All plasmids expressing the glutathione-S-transferase(GST)-human FCP1 fragments used for in vitro binding studies were constructed by PCR amplification using pJA533 as the template (*8*). The amplified DNA fragments were digested with *BamH*1 and *EcoR*1 and then inserted in frame into the *BamH*1 and *EcoR*1 sites of pGEX5X-1 (Amersham Biosciences, NJ). The pGEX2T expression vectors for HIV-1 Tat proteins (Tat_{1-86}, Tat_{1-72}, Tat_{1-48} and $Tat_{1-48C22G}$) (*48*) were obtained from the AIDS Research and Reference Reagent Program. The pGEX2T expression vector for HIV-1 Tat_{48-86} was constructed by PCR amplification of Tat cDNA using pGEX2T HIV-1 Tat_{1-86} as the template. The PCR fragments were then digested with *BamH*1 and *EcoR*1 and inserted in frame into the *BamH*1 and *EcoR*1 sites of the GST expression vector pGEX2T (Amersham Biosciences, NJ). An expression vector for the hexahistidine-(His_6)-Tat_{1-72} fusion protein was prepared by inserting a PCR-amplified Tat cDNA cut with *BglII* into the *BamH*1

site of pRSET-C (Invitrogen, CA). The expression vector for $RAP74_{436-517}$ has been described previously (*44*). The alanine substituted mutants GST-$FCP1_{879-961}$ (E956A and L957A) (*45*), GST-$FCP1_{562-738}$ and GST-$FCP1_{562-599}$ (Y592A and L593A), as well as the CK2 site mutant GST-$FCP1_{562-619}$ (T584E) were prepared by site-directed mutagenesis (Stratagene, CA). The expression vectors for preparing purified $FCP1_{562-619}$ and thioredoxin-His_6-$FCP1_{562-738}$ were created by inserting the *BamH*1 and *EcoR*1 fragments from pGEX5X-1 $FCP1_{562-619}$ and pGEX5X-1 $FCP1_{562-738}$, respectively, into the *BamH*1/*EcoR*1 sites of the pET-32c (Novagen, WI) expression vector. The pHIV+TARG400 template used for in vitro transcription experiments was generously provided by Q. Zhou and P. A. Sharp (*49*). The expression vector for the carboxyl-terminal histidine-tagged full-length hFCP1 was generously provided by Danny Reinberg. All plasmids created for this study were validated by DNA sequencing.

Immunodepletion of FCP1 from HeLa Nuclear Extract. Five hundred μL of HeLa nuclear extract prepared as previously described (*50*) were incubated with 1 μL of affinity-purified polyclonal FCP1 antibody or control IgG antibody (Sigma-Aldrich, MO) for 1 h at 4 °C. Extracts were loaded onto a 20 μL protein A-Sepharose columns that had been equilibrated with 400 μL BC100 buffer (20 mM Tris-HCl pH 7.9, 0.2 mM EDTA, 0.2 mM DTT, 20% glycerol and 100 mM KCl) (*51*) containing 250 mg/mL BSA prior to loading. The flow-through fractions were aliquoted and stored at −80 °C until needed for in vitro transcription assays with pHIV+TARG400.

In Vitro Transcription Assay. In vitro transcription reactions with Tat_{1-72} were performed as described previously (*49*, *52*) with some modifications. For each 25 μL reaction, we used 100 ng of supercoiled pHIV+TARG400 template, 30 μg of nuclear extract that was FCP1 or IgG depleted and various amounts of Tat_{1-72}. The His_6-Tat_{1-72} protein used for these studies was purified under denaturing conditions. The reactions were incubated at 30 °C for 30 min prior to the addition of 1 μL of [γ^{32}P]-CTP 3000 Ci/mM (Amersham Biosciences, NJ). The reactions were further incubated for 30 min and then stopped with the addition of 1 μL of 250 mM EDTA. Each reaction was then supplemented with 2 μL of RNAse T1 (5 U/μL) and incubated at 37 °C for 10 min. The G-less RNA transcripts were resolved on a denaturing polyacrylamide gel. Gels were vacuum-dried and ^{32}P-labeled RNA was detected by PhosphorImager analysis (Molecular Dynamics−Amersham Biosciences, NJ).

Yeast Two-Hybrid Assay. Yeast manipulations and growth media were described previously (*53*). To test the ability of yeast cells to grow on medium containing 3-aminotriazole (AT), 3 μL of a cell suspension (approximately 2,000 cells) were applied onto SD medium (BD Biosciences, NJ) containing 100 μg/mL adenine and 40 mM AT. As a control, a similar number of cells were applied onto medium lacking AT, but containing 100 μg/mL of adenine and histidine.

Protein Purification. The full-length FCP1 used for in vitro transcription of pHIV+TARG400 was purified from HeLa cells as described previously (*8*). The recombinant full-length His_6-tagged human FCP1 used for binding studies was purified from baculovirus-infected insect cells as described previously for yeast FCP1 (*19*). GST-FCP1 fragments were expressed in DH5α (Stratagene, CA). These cells were grown at 37 °C, and protein expression was induced with 0.7 mM isopropyl-β-D-thiogalactoside (IPTG) for 3 h at 30 °C. The cells were harvested and resuspended in EBC buffer (50 mM Tris-HCl pH 8.0, 120 mM NaCl, 0.5% NP-40 and 2 mM DTT) supplemented with protease inhibitors (Sigma, MO): 1 μg/mL leupeptin, 2 μg/mL aprotinin and 0.9 mg/mL PMSF. Cells were lysed by passage through a French press cell and centrifuged at 100,000 g for 40 min. The supernatant obtained from the high-speed centrifugation was added to glutathione(GSH)-Sepharose resin (Amersham Biosciences, NJ) and incubated with mixing at 4 °C for 30 min. The resin was collected by centrifugation and washed four times with wash buffer (50 mM Tris-HCl pH 8.0, 100 mM NaCl, 1 mM EDTA, 0.5% NP-40, 0.05% SDS and 1 mM DTT). GST-FCP1 fragments were eluted off the resin with 15 mM reduced glutathione (Sigma, MO) for 10 min at 25 °C, dialyzed into protein storage buffer (50 mM Tris-HCl pH 8.0, 100 mM NaCl, 2 mM DTT and 20% glycerol), aliquoted and stored at −80 °C. GST-FCP1 fragments were rebound to fresh GSH-Sepharose resin prior to protein−protein binding studies.

All HIV-1 Tat proteins used for binding studies were expressed as GST-Tat constructs and purified as stated for the GST-FCP1 fragments up to the elution step. At this step, Tat proteins were cleaved from the GST using thrombin (Calbiochem, CA) and subsequently dialyzed into 5% acetic acid and loaded on a C-4 reverse-phase HPLC column (Vydac, CA). Tat proteins were eluted from the column using an acetonitrile gradient (25% to 45% over 20 min) in 0.05% TFA at a flow rate of 8 mL/min. Purified Tat proteins were stored lyophilized in aliquots at −20 °C. The GST-Tat_{1-86} used in binding studies with His_6-tagged FCP1 was purified as described for GST-FCP1 fragments up to the end of the high-speed centrifugation step. The supernatant from the high-speed centrifugation was snap frozen in liquid nitrogen and stored at −80 °C until needed. Prior to each experiment, this partially purified GST-Tat_{1-86} was freshly purified by capture and washes on GSH-Sepharose resin as described for the GST-FCP1 fragments.

The $RAP74_{436-517}$ was purified as described previously (*44*). The FCP1 peptides ($FCP1_{579-600}$ and $FCP1_{583-607}$) used for the protein−protein binding studies and for the 2D ^{1}H-^{15}N heteronuclear single quantum coherence (HSQC) spectrum were chemically synthesized at the Medical College of Georgia with an extra glycine residue at the amino terminus. The peptides were purified to homogeneity on a C-4 reverse-phase HPLC column using an acetonitrile gradient (30% to 50% over 20 min) in 0.05% TFA at a flow rate of 8 mL/min. The purified $FCP1_{579-600}$ and $FCP1_{583-607}$ peptides were stored lyophilized in aliquots at −20 °C.

The thioredoxin-His_6-$FCP1_{562-738}$ fusion protein used for in vitro binding studies was obtained by expression in BL21-(DE3). The cells were induced with 1 mM IPTG for 4 h at 37 °C. The cells were harvested, lysed by passage though a French press in PE buffer (25 mM phosphate pH 7.2 and 1 mM EDTA) and centrifuged at 15,000 g for 30 min. The pellet, which contained the protein in an inclusion body, was washed twice at 25 °C in PE buffer supplemented with 1 M urea and 0.5% Triton X-100 to remove contaminants. The washed pellet was then solubilized in 6 M guanidinium HCl and 10 mM Tris pH 8.0 buffer for 15 min at 50 °C and centrifuged at 100,000 g for 40 min at 4 °C. The fusion

protein from the high-speed supernatant was first bound to Ni^{2+}-charged Chelating Sepharose Fast Flow resin (Amersham Biosciences, NJ). The captured fusion protein was gradually refolded on the resin at 25 °C by stepwise incubation in refolding buffer A (10 mM Tris pH 8.0, 500 mM NaCl, 20% glycerol and 1 mM β-mercaptoethanol) supplemented with 4, 2, and 1 M urea. The fusion protein was eluted from the resin using 250 mM imidazole in phosphate buffered saline, dialyzed overnight into protein storage buffer and aliquots were stored at −80 °C. The $FCP1_{562-619}$ protein used in the CK2 assay was obtained by expression of a thioredoxin-His_6-$FCP1_{562-619}$ fusion protein in BL21(DE3). The cells were induced with 1 mM IPTG for 4 h at 37 °C. The thioredoxin-His_6-$FCP1_{562-619}$ was purified from the inclusion body under denaturing conditions as described for the thioredoxin-His_6-$FCP1_{562-738}$. After the high-speed centrifugation, the fusion protein from the supernatant was refolded by stepwise dialysis at 4 °C in refolding buffer A supplemented with 4, 2, and 1 M urea and finally in phosphate buffered saline. $FCP1_{562-619}$ was then cleaved from thioredoxin-His_6 with thrombin (Calbiochem, CA). The $FCP1_{562-619}$ protein was applied to a Q-Sepharose High Peformance (Amersham Biosciences, NJ) column (100 mL bed volume) equilibrated with buffer A (20 mM phosphate buffer pH 7.2, 1 mM DTT and 1 mM EDTA). $FCP1_{562-619}$ was eluted from the column using a gradient (from 0% to 100% over 700 mL) of buffer B (20 mM phosphate pH 7.2, 1 mM DTT, 1 mM EDTA and 1 M NaCl) and dialyzed overnight at 4 °C into 3% acetic acid. The eluent volume was reduced using a rotovap, and $FCP1_{562-619}$ was applied to a C-4 reverse-phase HPLC column (Vydac,CA). $FCP1_{562-619}$ was eluted from this column using an acetonitrile gradient (30% to 50% over 20 min) in 0.05% TFA at a flow rate of 8 mL/min. Eluted $FCP1_{562-619}$ was dialyzed overnight into protein storage buffer, and aliquots were stored at −80 °C. Protein concentrations were estimated using a combination of UV spectroscopy at 280 nm (*54*) and comparison with known amounts of bovine serum albumin (Promega) on Coomassie blue-stained gels.

Protein−Protein Binding Assay. For all in vitro binding experiments with immobilized GST-FCP1 we used the following procedure. GST-FCP1 fragments were first coupled to 10 μL of GSH-Sepharose resin (Amersham Biosciences, NJ) in 500 μL of EBC buffer for 1 h. The bound GST-FCP1 was then collected by centrifugation, washed with EBC buffer and equilibrated with binding buffer PP (40 mM HEPES pH 7.9, 120 mM NaCl, 0.5% NP-40 and 10 mM DTT). The binding reactions contained equimolar amounts of various GST-FCP1 fragments and purified HIV-1 Tat proteins (0.5 μM Tat_{1-86}, Tat_{1-72}, Tat_{1-48}, $Tat_{1-48C22G}$ or Tat_{48-86}) or $RAP74_{436-517}$ (10 μM). Binding reactions were performed in 500 μL of binding buffer PP at 4 °C for 1 h. For binding with Tat proteins, this buffer was supplemented with 80 μM zinc sulfate. The protein−protein complexes were collected by centrifugation and then washed (2 to 4 times) with binding buffer supplemented with 350 mM NaCl (for binding assays including RAP74 no additional salt was added). The washed pellet was resuspended in NuPage LDS 4X sample buffer (Invitrogen, CA), and proteins were resolved on a 12% Bis-Tris NuPage gel using 1X MES electrophoresis buffer (Invitrogen, CA). Proteins were transferred to a PVDF membrane (Millipore, MA) using the Invitrogen transfer system. The Tat_{1-72}, Tat_{1-48} and $Tat_{1-48C22G}$ proteins were detected using a 1:1,000 dilution of the Tat monoclonal antibody (15.1) and a 1:10,000 dilution of anti-mouse horseradish peroxidase (HRP) conjugated secondary antibody. Tat_{48-86} was detected using a 1:5,000 dilution of the Tat polyclonal antibody (705) and a 1:20,000 dilution of the anti-rabbit HRP conjugated secondary antibody. The $RAP74_{436-517}$ protein was detected using a 1:400 dilution of the RAP74 polyclonal antibody C-18 and a 1:7,000 dilution of anti-rabbit HRP conjugated secondary antibody.

For binding reactions with immobilized GST-Tat (Figure 4A), control GST or GST-Tat_{1-86} were purified on GSH-Sepharose as described above. Binding experiments were performed in 500 μL of binding buffer PP containing 0.5 μM purified His_6-$FCP1_{1-961}$ or thioredoxin-His_6-$FCP1_{562-738}$ and 0.5 μM GST-Tat_{1-86}. Bound His_6-FCP1 proteins were collected and washed (2 to 4 times) in binding buffer PP supplemented with 350 mM NaCl. The washed pellet was resuspended in NuPage LDS 4X sample buffer, and proteins were resolved on a NuPage 4−12% Bis-Tris gradient gel in 1X MES electrophoresis buffer. Proteins were transferred to an Immobilon-P membrane (Millipore, MA) and detected using a 1:1,000 dilution of a His_6 monoclonal antibody (Novagen, WI) and a 1:10,000 dilution of an HRP-conjugated secondary antibody. The bound secondary antibodies were detected by chemiluminescence using the ECL-Plus kit (Amersham Biosciences, NJ), and all membranes were subsequently stained with Coomassie blue to verify equivalent GST-fusion protein input.

NMR Spectroscopy. The ^{15}N-labeled $RAP74_{436-517}$ was expressed from a pGEX2T vector (Amersham Biosciences, NJ) in BL21(DE3). Labeled protein was obtained by growth in a modified minimal medium containing ^{15}N-labeled NH_4Cl as the sole source of nitrogen (*44*). The NMR sample consisted of 1 mM ^{15}N-labeled $RAP74_{436-517}$/1 mM unlabeled $FCP1_{579-600}$ in 500 μL of 20 mM sodium phosphate pH 6.5 and 1 mM EDTA (90% H_2O and 10% D_2O). The 2D ^{1}H-^{15}N HSQC (*55*) was collected at 27 °C using Varian ^{Unity}Inova 600 MHz NMR spectrometer equipped with a z pulsed-field gradient unit and a HCN triple resonance probe. The NMR data was processed with the NMRPipe/NMRDraw package (*56*).

Phosphorylation of FCP1 Fragments with CK2. For phosphorylation of FCP1, the $FCP1_{562-619}$ protein (or control protein) was first diluted at 1.25 mg/mL in 20 μL of 1.25X phosphorylation buffer (20 mM Tris-HCl pH 7.5, 25 mM KCl, 10 mM $MgCl_2$, 350 μM ATP and 2.5 μCi [γ^{32}P]-ATP (4500 Ci/mmol)). The reaction was initiated by the addition of 10 units (5 μL) of CK2 enzyme (New England Biolabs, MA) diluted in CK2 buffer (20 mM Tris-HCl pH 7.5, 200 mM NaCl, 0.5 mM DTT, 10% glycerol and 0.5% Triton X-100). The phosphorylation reactions were incubated at 25 °C for 30 min and terminated by the addition of NuPage LDS 4X sample buffer. For mock phosphorylation, the reaction was performed similarly, but 1X CK2 buffer replaced the CK2 enzyme. Proteins were resolved on 12% Bis-Tris NuPage gels using 1X MES electrophoresis buffer (Invitrogen, CA). The phosphorylated proteins were detected by PhosphorImager analysis (Molecular Dynamics-Amersham Pharmacia, NJ). Phosphorylation of the GST-FCP1 fusion protein used in protein−protein binding assays was

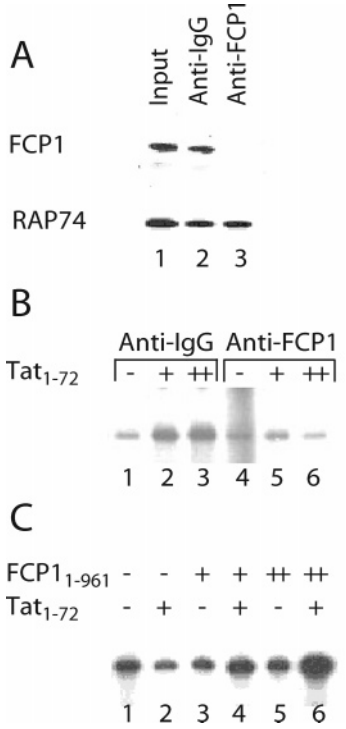

FIGURE 1: FCP1 mediates transcriptional activation by HIV-1 Tat in vitro. (A) Immuno-depletion of endogenous FCP1. HeLa cell nuclear extracts (30 μg) depleted with control IgG (lane 1) or affinity-purified FCP1 polyclonal (lane 2) antibodies were analyzed by western blot using FCP1 and RAP74 antibodies. (B) Effect of FCP1 depletion on transcription activated by Tat. Nuclear extracts depleted with control IgG (lanes 1−3) or FCP1 affinity-purified antibodies (lanes 4−6) were tested for their ability to support transcription from the pHIV+TARG400 template in the absence (−) or presence of 200 ng (+) or 400 ng (++) Tat_{1-72}. (C) Restoration of Tat activation in nuclear extracts treated with FCP1 affinity-purified antibody after the addition of full-length purified FCP1. In vitro transcription reactions were performed with nuclear extracts treated with FCP1 affinity-purified antibody in the absence (−) or presence (+) of 200 ng Tat_{1-72} and either 0.25 μL (+) or 0.5 μL (++) of full-length FCP1 (Mono Q fraction 34 provided by M. Dahmus) (*8*).

obtained by capturing GST-$FCP1_{562-619}$ (or control GST) on GSH-Sepharose resin and exchanging into CK2 phosphorylation buffer. Following the CK2 phosphorylation reaction, the resin was washed (2 to 4 times) in binding buffer PP.

RESULTS

FCP1 Is Required for Tat-Activated Transcription in Vitro. Although previous studies have shown that Tat is capable of inhibiting the phosphatase activity of FCP1 in vitro (*40*), it has not yet been determined if FCP1 is required for Tat-mediated transcriptional activation. To address this question, in vitro transcription assays using pHIV+TARG400 as a template were performed with nuclear extracts that were either depleted of FCP1 with anti-FCP1 antibodies, or mock depleted with nonspecific anti-IgG antibodies (Figure 1). As shown in Figure 1A, HeLa cell nuclear extracts could be completely depleted of FCP1 using anti-FCP1 antibodies prior to the transcription assays. In the presence of HeLa cell nuclear extract containing FCP1 (IgG-depleted extract) there was an increase in pHIV+TARG400 transcription with increasing concentration of Tat (Figure 1B, lanes 1−3). However, in the presence of FCP1-depleted extracts there was no increase in pHIV+TARG400 transcription with increasing concentration of Tat (Figure 1B, lanes 4−6). When purified FCP1 was added back to the transcription reaction, we observed an increase in transcription from the pHIV+TARG400 template in the presence of Tat (Figure 1C). The immunodepletion of FCP1 from nuclear extracts did not remove RAP74 (Figure 1A). Furthermore, it is unlikely that immunodepletion of FCP1 removed the RNAPII holoenzyme from the HeLa nuclear extract since the levels of human SRB7, an intrinsic component of the holoenzyme, are similar in both IgG-depleted and FCP1-depleted extracts (data not shown). Therefore, the reduction in Tat-activated transcription in the FCP1-immunodepleted extracts is not due to removal of either RAP74 or RNAPII. Since the HIV-1 promoter of the pHIV+TARG400 template contains binding sites for Sp1, which are important for activation by Tat (*57*, *58*), we wanted to verify if depletion of FCP1 had any effect on Sp1-activated transcription. In the presence of FCP1-depleted extract there was essentially no change in pHIV+TARG400 transcription compared to the IgG-depleted extract (Figure 1B, lanes 1 and 4), suggesting that FCP1 depletion did not affect Sp1-activated transcription.

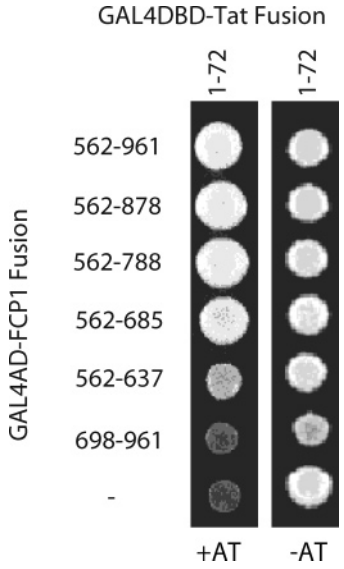

FIGURE 2: FCP1 and HIV-1 Tat interact in the yeast two-hybrid system. *S. cerevisiae* cells were co-transformed with plasmids expressing FCP1 fragments fused to the GAL4 activation domain (GAL4AD) and a plasmid expressing Tat_{1-72} fused to the GAL4 DNA-binding domain (GAL4DBD). For each of the resulting strains, a drop of a cell suspension was applied onto SD medium containing (+AT) or lacking (-AT) 3-aminotriazole and allowed to grow at 30 °C for 4 days. The amino acid numbering for FCP1 is given according to GenBank accession number NP_004706.2.

FCP1 Interacts with HIV-1 Tat in the Yeast Two-Hybrid System. Yeast-two hybrid studies were performed using various fragments of human FCP1 fused to the GAL4 activation domain and HIV-1 Tat_{1-72} fused to the GAL4 DNA-binding domain (Figure 2). These studies initially demonstrated that Tat_{1-72} interacts with a carboxyl-terminal fragment of human FCP1 ($FCP1_{562-961}$). Shorter carboxyl-terminal fragments of FCP1 spanning amino acids 562−878, 562−788 and 562−685 were also capable of interacting with Tat. An even shorter carboxyl-terminal fragment, $FCP1_{562-637}$, leads to a less robust growth signal that is comparable to the control yeast grown in the absence of 3-aminotriazole (AT) (Figure 2). This result is consistent with $FCP1_{562-637}$ being impaired for Tat binding and indicates that $FCP1_{562-685}$

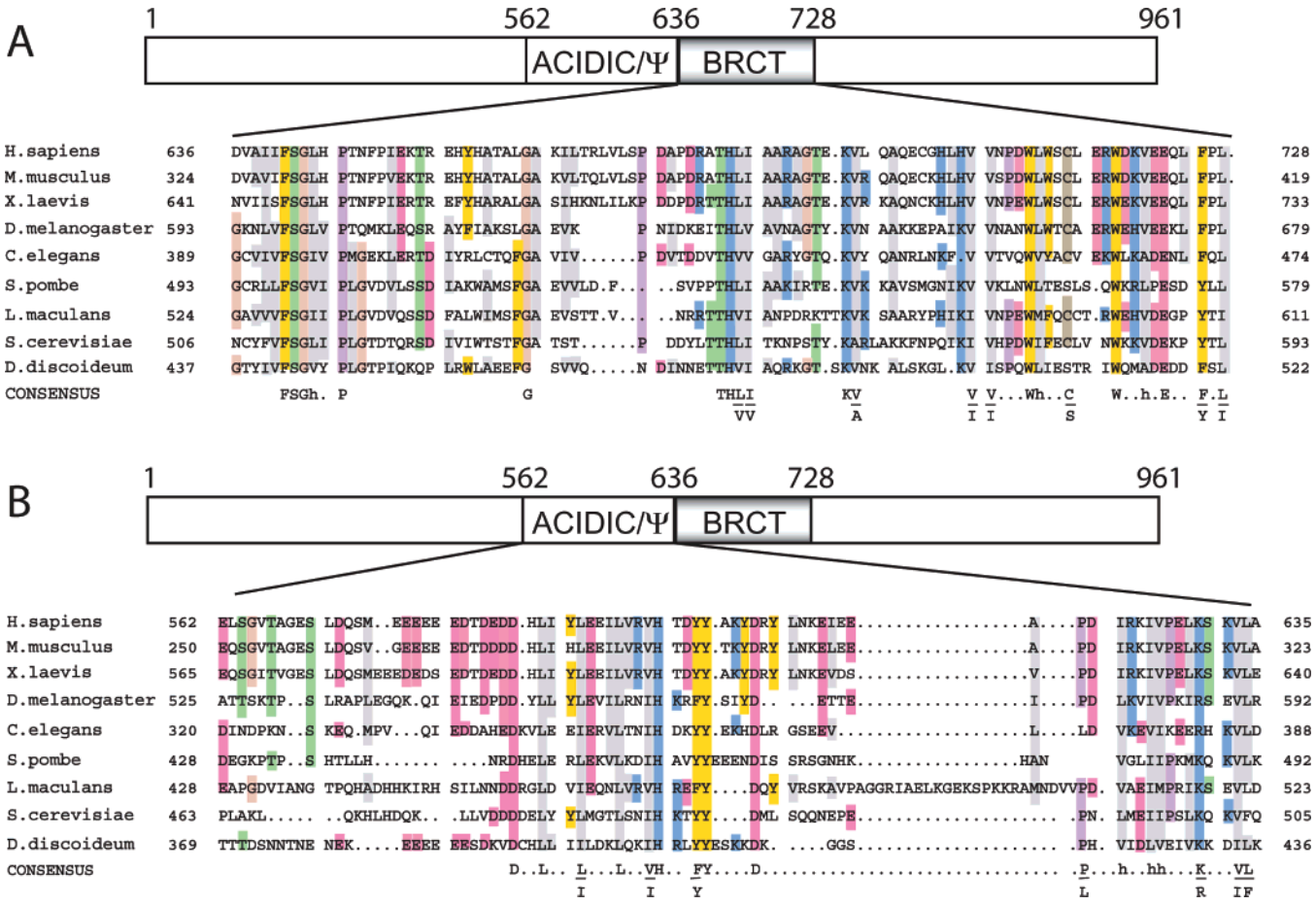

FIGURE 3: The FCP1 central domain is conserved in eukaryotes. The sequences of (A) the BRCT and (B) the acidic/hydrophobic regions of FCP1 from *Homo sapiens* (NP_004706.2), *Mus musculus* (AAH53435), *Xenopus laevis* (AAK27686), *Drosophila melanogaster* (Q9W147), *Caenorhabditis elegans* (NP_492423), *Schizosaccharomyces pombe* (Q9P376), *Leptosphaeria maculans* (AAM81360), *Saccharomyces cerevisiae* (NP_014004) and *Dictyostelium discoideum* (AAM33170) were aligned using Pfam (*59*) and BLAST (*60*). The numbers in parentheses are GenBank accession numbers, except for *D. melanogaster*'s number, which is from the Swiss Protein Database. Residues conserved in at least four species are highlighted using the following color code; pink, acidic residues (D, E); sky blue, basic residues (H, K, R); gray, hydrophobic residues (A, I, L, M, V); gold, aromatic residues (F, Y, W); green, threonine and serine residues (T, S); peach, glycine residues (G); purple, proline residues (P) and beige, cysteine residues (C). A consensus is provided for residues that are conserved in all species.

is the smallest region that binds to Tat in the yeast two-hybrid system. However, one has to be aware that a weaker signal in the yeast two-hybrid system is not necessarily indicative of a decrease in binding affinity; a weaker signal can be brought about by other factors such as differences in protein expression levels, folding and/or localization. Finally, a fragment encompassing the carboxyl-terminal 264 amino acids of FCP1, $FCP1_{698-961}$, was unable to bind to Tat. It therefore appears that the central domain of FCP1 ($FCP1_{562-685}$), which is essential for cell viability and phosphatase activity (*21*), is also sufficient for Tat binding in yeast two-hybrid studies (Figure 2).

Sequence Conservation in the Central Domain of FCP1. Prior to initiating in vitro binding studies with purified human FCP1 fragments, conserved amino acid regions within the central domain of FCP1 were identified using Pfam (*59*) and BLAST (*60*) searches (Figure 3). The boundaries of the BRCT domain ($FCP1_{636-728}$) were initially defined with the Pfam multiple alignment program (data not shown) (*59*). We found that the BRCT domain of human FCP1 is defined by amino acids 636 to 728 (Figure 3A). The BRCT domains of published FCP1 sequences were subsequently aligned with BLAST (Figure 3A). The percentage of sequence identity to human FCP1 within the BRCT domain is very high for *Mus musculus* (95%) and *X. laevis* (80%) and lower (27% to 42%) for other eukaryotic sequences (Figure 3A). Interestingly, the region of FCP1 located immediately at the amino-terminus of the BRCT domain ($FCP1_{562-635}$) also showed considerable sequence identity among eukaryotic FCP1 proteins. We defined this region as the acidic/hydrophobic region of FCP1 ($FCP1_{562-635}$) based on the high occurrence of acidic and hydrophobic amino acids. The percentage of sequence identity to human FCP1 within the acidic/hydrophobic region is also very high for *M. musculus* (91%) and *X. laevis* (84%) and lower (23% to 38%) for other eukaryotic sequences (Figure 3B).

BRCT and Acidic/Hydrophobic Domains of FCP1 Bind Directly to HIV-1 Tat in Vitro. The yeast two-hybrid results revealed that a minimal FCP1 fragment including residues 562 to 685 is sufficient for binding to HIV-1 Tat_{1-72}. We attempted to confirm and extend these results in vitro, using purified proteins and protein fragments (Figures 4 and 5) in batch-affinity binding assays. Initial binding experiments were performed using His_6-tagged $FCP1_{1-961}$ and thioredoxin-His_6-$FCP1_{562-738}$ to compare the relative binding of these proteins to GST-Tat_{1-86} immobilized on GSH-Sepharose

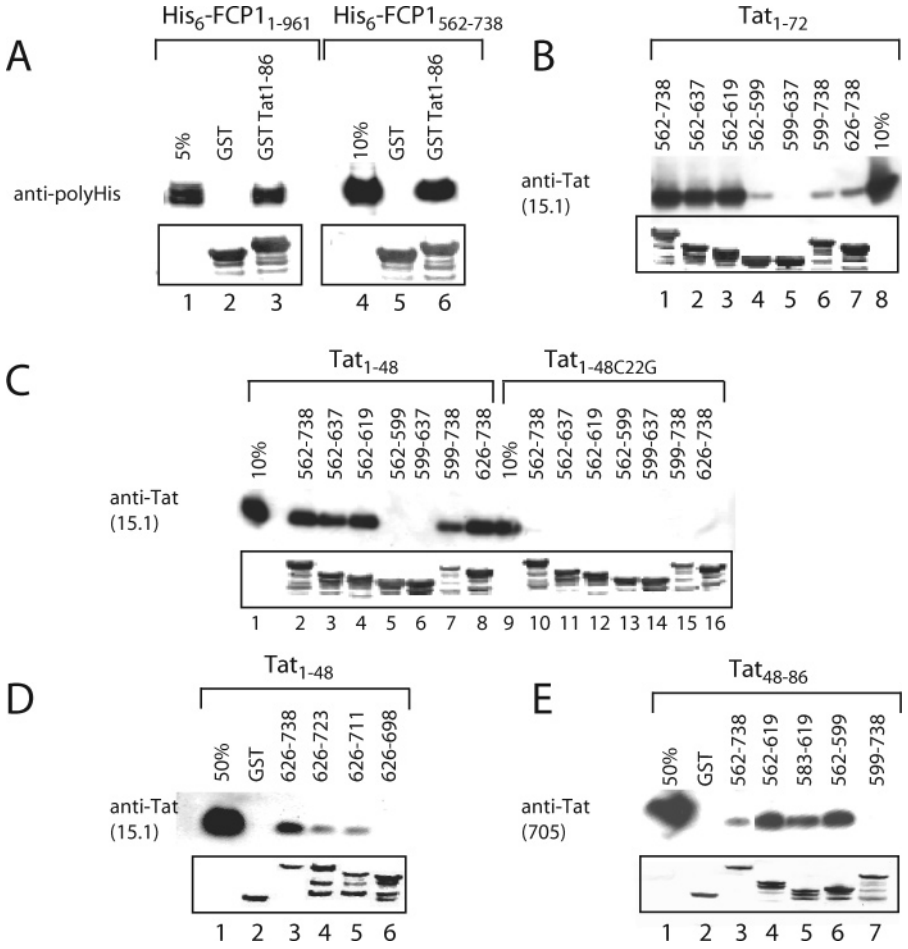

FIGURE 4: Identification and characterization of the Tat-binding regions of FCP1 using in vitro binding studies. (A) Recombinant full-length His_6-FCP1 and thioredoxin-His_6-$FCP1_{562-738}$ interact similarly with GST-Tat_{1-86}. GST-Tat_{1-86} was coupled to GSH-Sepharose and incubated with recombinant His_6-$FCP1_{1-961}$ or thioredoxin-His_6-$FCP1_{562-738}$ (5% His_6-FCP1 and 10% $FCP1_{562-738}$ inputs are shown). Bound FCP1 was detected using a polyhistidine monoclonal antibody. (B) Interaction of purified HIV-1 Tat_{1-72} with various GST-FCP1 fragments reveals two Tat-binding regions in FCP1. GST-FCP1 fusion proteins were coupled to GSH-Sepharose resin and incubated with purified HIV-1 Tat_{1-72} (10% of the Tat_{1-72} input is shown). Bound Tat protein was detected using the Tat monoclonal antibody (15.1). (C) The HIV-1 Tat activation domain (Tat_{1-48}) interacts specifically with two regions of FCP1. Purified HIV-1 Tat_{1-48} or purified HIV-1 $Tat_{1-48C22G}$ were incubated with various GST-FCP1 fragments (10% inputs for each Tat fragment are shown). Bound wild-type and C22G mutant Tat_{1-48} proteins were detected using the Tat monoclonal primary antibody (15.1), which recognizes amino acids 1−16 of HIV-1 Tat. (D) The carboxyl-terminal region of the FCP1 BRCT domain is essential for interaction with Tat_{1-48}. Purified HIV-1 Tat_{1-48} protein was added to various carboxyl-terminal BRCT deletion fragments of GST-$FCP1_{626-738}$ (50% Tat_{1-48} input is shown). Bound Tat_{1-48} protein was detected using the Tat monoclonal (15.1) primary antibody. (E) The arginine-rich carboxyl terminus of HIV-1 Tat_{48-86} interacts with the acidic/hydrophobic region of the central domain of FCP1. Purified Tat_{48-86} was incubated with various GST-FCP1 fragments (50% Tat_{48-86} input is shown). Tat_{48-86} protein was detected using the Tat polyclonal primary antibody (705). For all batch-affinity protein-binding assays (Figures 4A-E, 6B−D, 8A−C and 9B), figures are shown as follows. The vertical labels above each lane indicate the GST or GST-fusion protein bound to the GSH-Sepharose resin, the horizontal labels above the lanes indicate the free protein added to the resin in the binding assay, and the labels on the left of the figure indicate the antibody used to detect the free protein retained in the assay. In control lanes, a given percentage of the free protein input in the reaction was directly loaded on the gel, and this percentage is indicated vertically above these lanes. For GST-FCP1 fragments, only the numbering defining these fragments are indicated. Equivalent inputs of GST, GST-Tat or GST-FCP1 fusion proteins were determined by performing a Coomassie blue stain of the membrane and are shown in the boxed region.

beads. In this assay, His_6-$FCP1_{1-961}$ (Figure 4A, lanes 1−3) and thioredoxin-His_6-$FCP1_{562-738}$ (Figure 4A, lanes 4−6) appear to bind similarly to Tat_{1-86}. These results confirm the yeast two-hybrid finding that the central domain of FCP1 is sufficient for interaction with the Tat protein.

Several carboxyl- and amino-terminal truncated versions of $FCP1_{562-738}$ were then purified as GST-fusion proteins from *E. coli* and assayed for Tat_{1-72} binding using our in vitro batch-affinity binding assay. Carboxyl-terminal deletion fragments $FCP1_{562-637}$ and $FCP1_{562-619}$ retained the same level of binding to Tat_{1-72} as $FCP1_{562-738}$ (Figure 4B, lanes 1−3). However, with $FCP1_{562-599}$ less binding to Tat_{1-72} was observed (Figure 4B, lane 4), indicating that $FCP1_{562-619}$, which comprises most of the acidic/hydrophobic region, is a minimal Tat binding domain. Since deletions of FCP1 residues 599 to 619 caused a drastic change in binding, we tested the binding of Tat_{1-72} to GST-$FCP1_{599-637}$ (Figure 4B, lane 5). Since no binding was detected with this fragment, we concluded that although residues 599−619 are important, they are not sufficient for binding. Amino-terminal deletion fragments of $FCP1_{562-738}$, $FCP1_{626-738}$ and $FCP1_{599-738}$ also bound Tat, although poorly (Figure 4B, lanes 6−7), indicating that $FCP1_{626-738}$, which contains the BRCT domain, binds independently to Tat_{1-72}, but likely with lower affinity than the central domain of FCP1. Similar results were obtained using Tat_{1-86} instead of Tat_{1-72} (data not shown). These

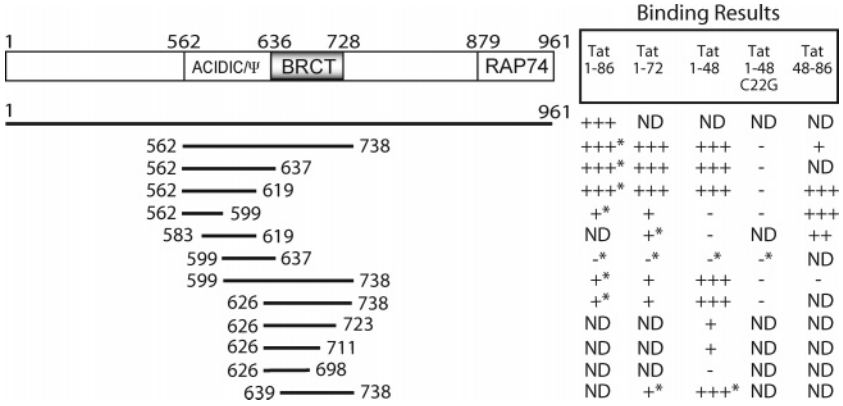

FIGURE 5: Summary of the interactions of HIV-1 Tat proteins with various GST-FCP1 fragments. Strong (+++), medium (++), weak (+) and no (−) binding was detected between Tat proteins and GST-FCP1 fragments. ND means not determined, and * indicates that the results have been obtained but are not explicitly shown.

binding studies reveal that there are two non-overlapping Tat binding sites in the central domain of FCP1, one located within the acidic/hydrophobic region (562−619), and the other within the 626−738 fragment that contains the BRCT domain (636−728).

Additional binding studies were performed using Tat_{1-48} or a transactivation-negative C22G mutant of Tat_{1-48} (*40*, *61*) and the same GST-FCP1 deletion fragments used with Tat_{1-72} (Figure 4C). The Tat_{1-48} fragment contains only the activation domain, but not the arginine-rich and glutamine-rich regions present in residues 48−72 of Tat (*62*). The binding results with Tat_{1-48} were similar to those obtained with Tat_{1-72}, with the exception that Tat_{1-48} bound more strongly than Tat_{1-72} to $FCP1_{626-738}$ and $FCP1_{599-738}$ (Figure 4C, lanes 1−8), perhaps because Tat residues 48−86 prevent an optimal interaction of Tat_{1-48} with the BRCT domain ($FCP1_{636-728}$). Indeed, a negative effect of residues 48−86 on the activity of the amino-terminal activation domain has been noted previously ((*63*) and our own unpublished studies). Binding was not observed between the transactivation-negative C22G mutant of Tat_{1-48} ($Tat_{1-48C22G}$) and any of the GST-FCP1 fragments (Figure 4C, lanes 9−16), suggesting that the interactions with wild-type Tat proteins are specific.

To further explore the interaction of Tat_{1-48} with the BRCT domain of FCP1, several deletion fragments of GST-$FCP1_{626-738}$ were purified and used for in vitro binding studies with purified Tat_{1-48} (Figure 4D). An amino-terminal deletion fragment of the FCP1 BRCT domain (GST-$FCP1_{639-738}$) was tested for Tat_{1-48} binding. This shorter BRCT fragment binds Tat_{1-48} as well as GST-$FCP1_{626-738}$ (data not shown). However, we detected little binding with $FCP1_{626-723}$ and $FCP1_{626-711}$, and no binding with $FCP1_{626-698}$, indicating that the carboxyl-terminal portion of the BRCT domain (698−738) is essential for optimal Tat_{1-48} binding. Although truncation of the BRCT domain may destabilize the overall fold of the protein fragment, the carboxyl-terminal deletions used in this study were planned using a predicted secondary structure alignment to minimize truncations within a secondary structure element (data not shown) (*64*).

We noted another difference in the binding results between full-length Tat and Tat_{1-48}, which is that Tat_{1-72} (Figure 4B, lane 4) and Tat_{1-86} (not shown) interact weakly with GST-$FCP1_{562-599}$, whereas no such interaction was observed for Tat_{1-48} (Figure 4C, lane 5). These results raised the possibility that a weak binding site for the carboxyl-terminal region of Tat (Tat_{48-86}) might be present within $FCP1_{562-599}$. To further investigate this possibility, the Tat_{48-86} fragment was purified and used in binding studies with various GST-FCP1 fragments (Figure 4E). Binding was not detected between Tat_{48-86} and the BRCT-containing fragment $FCP1_{599-738}$ (Figure 4E, lane 7). Rather, Tat_{48-86} only bound to FCP1 fragments $FCP1_{562-619}$, $FCP1_{583-619}$, and $FCP1_{562-599}$ that contained the acid-rich portion of the acidic/hydrophobic region (Figure 4E, lanes 3−6). This is perhaps not surprising given that Tat_{48-86} is positively charged. Unexpectedly, the binding of Tat_{48-86} to GST-$FCP1_{562-738}$ was weaker than the binding to GST-$FCP1_{562-599}$ (Figure 4E, lanes 3 and 6), a result consistent with the notion that intramolecular interactions between the acidic/hydrophobic region and the BRCT domain prevent optimal binding of Tat_{48-86} (see Discussion). Finally, we also noted that in contrast to Tat_{1-72}, which binds well to GST-$FCP1_{562-738}$ (Figure 4B, lane 1) but poorly to GST-$FCP1_{562-599}$ (Figure 4B, lane 4), Tat_{48-86} behaved in the reverse manner, binding better to GST-$FCP1_{562-599}$ (Figure 4E, lane 3) than to GST-$FCP1_{562-738}$ (Figure 4E, lane 6). These results are consistent with the notion that the positively charged 48−86 region of Tat does not interact optimally with the acid-rich $FCP1_{562-599}$ in the context of the full-length Tat protein, and, if so, provides further evidence for an antagonistic interplay between the Tat activation and basic domains (see Discussion). A summary of the in vitro binding results between Tat and GST-FCP1 fragments is presented in Figure 5.

The Acidic/Hydrophobic Region within the Central Domain of FCP1 Also Binds to the Carboxyl-Terminal Domain of RAP74. A small conserved acidic/hydrophobic sequence motif located within the carboxyl-terminal region of FCP1 ($FCP1_{879-961}$), has been shown to be important for mediating interactions between FCP1 and the carboxyl-terminal domain of RAP74 ($RAP74_{436-517}$) (*45*). The consensus sequence of this motif in $FCP1_{879-961}$ was derived from vertebrates and yeast sequences as D/EXD/EDEXXXXLIEXELXDhh (*45*). Interestingly, we found that a similar acidic/hydrophobic sequence is present in the central domain of human FCP1 ($FCP1_{562-635}$), from approximately residues 578 to 605 (Figures 3B and 6A), thereby raising the possibility that this second motif might also be involved in RAP74 binding. This acidic/hydrophobic motif in the central domain of FCP1 appears to be highly conserved among vertebrates (*H.*

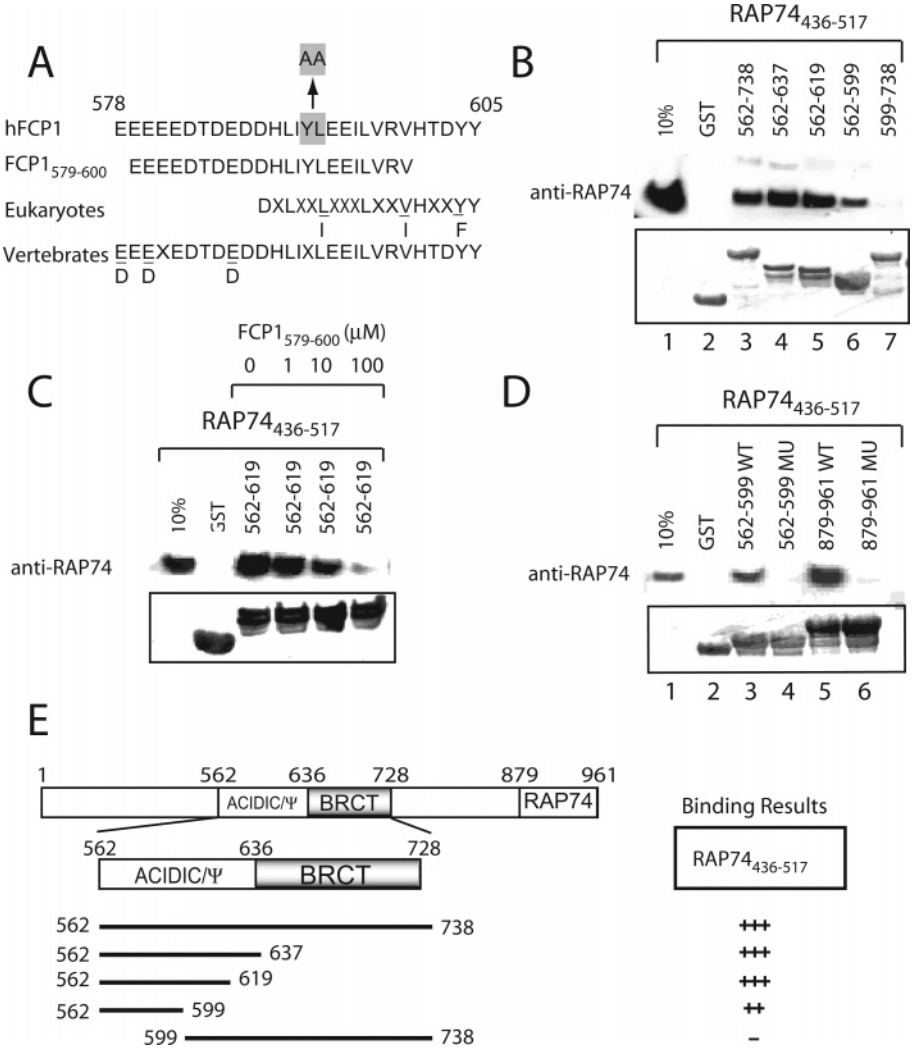

FIGURE 6: RAP74 interacts with a small conserved acidic/hydrophobic motif in the central domain of FCP1. (A) Region of human FCP1 (amino acids 578−605), which contains a conserved acidic/hydrophobic motif and consensus sequences from eukaryotes and vertebrates (See Figure 3B). The location of the Y592A/L593A mutation and the sequence $FCP1_{579-600}$ are also shown. (B) Interaction of $RAP74_{436-517}$ with various GST-FCP1 fragments. GST-FCP1 fragments were coupled to GSH-Sepharose resin and incubated with purified $RAP74_{436-517}$ (10% $RAP74_{436-517}$ input is shown). (C) A small peptide derived from FCP1 ($FCP1_{579-600}$) interacts with $RAP74_{436-517}$. GST-$FCP1_{562-619}$ (10 μM) and purified $RAP74_{436-517}$ (10 μM) proteins were incubated in the presence of increasing amounts of $FCP1_{579-600}$ (0, 1, 10 and 100 μM). (D) Alanine substitutions within the conserved hydrophobic motif inhibit RAP74 binding to the central domain of FCP1. We examined the interaction of $RAP74_{436-517}$ with the GST-$FCP1_{562-599}$ Y592A/L593A mutant (562−599 MU) and compared with the wild-type $FCP1_{562-599}$ (562−599 WT). As a control we repeated the binding experiment of $RAP74_{436-517}$ with GST-$FCP1_{879-961}$ E956A/L957A mutant (879−961 MU) and the wild-type GST-$FCP1_{879-961}$ (879−961 WT) (*45*). Figures (B)−(D) are shown as described in the legend of Figure 4, and for these experiments bound $RAP74_{436-517}$ was detected using the RAP74 polyclonal antibody (C-18). (E) Summary of the $RAP74_{436-517}$ interactions with various GST-FCP1 fragments. Strong (+++), medium (++) and no (−) binding was detected between $RAP74_{436-517}$ and GST-FCP1 fragments.

sapiens, *M. musculus* and *X. laevis*) (Figure 3), but less so among other eukaryotic sequences. Based on the sequence conservation (Figure 3B), we defined the consensus DXLXXL/IXXXLXXV/IHXXF/YY for eukaryotes and a more refined consensus, E/DEE/DXEDTDE/DDDHLIXLEEILVRVHTDYY, specifically for vertebrates (Figure 6A).

In vitro binding studies were used to define the minimal RAP74-binding site within the central domain of FCP1 (Figure 6B). Purified $RAP74_{436-517}$ was used in batch-affinity binding assays together with various GST-FCP1 fragments. FCP1 fragments that contain the small acidic/hydrophobic motif ($FCP1_{562-738}$, $FCP1_{562-637}$ and $FCP1_{562-619}$) interacted with $RAP74_{436-517}$ (Figure 6B, lanes 3−6), whereas GST-$FCP1_{599-738}$, which lacks this motif, did not (Figure 6B, lane 7).

The small peptide $FCP1_{579-600}$, which contains the small acidic/hydrophobic motif sequence (Figure 6A and 6C) was chemically synthesized and used as a competitor in our binding assay. $FCP1_{579-600}$ substantially inhibited the interaction between GST-$FCP1_{562-619}$ and $RAP74_{436-517}$ at concentrations (1−10 μM) similar to those of the other proteins in this assay (Figure 6C). Another small peptide, $FCP1_{583-607}$, which spans the small acidic/hydrophobic motif but contains additional conserved residues, was also synthesized. However, because of its poor solubility in aqueous solution, this peptide could not be used reliably in binding studies. Therefore, $FCP1_{579-600}$ represents the minimal conserved RAP74-binding site that we could define within the central domain of FCP1.

The small hydrophobic motifs located within the central and carboxyl-terminal domains of FCP1 resemble the LXXLL motifs found in members of the steroid hormone receptor superfamily (*45*). We previously examined the requirement of the first conserved leucine of the LXXLL-like motif of the carboxyl-terminus of FCP1 and found that replacement of this leucine and its preceding residue by alanines significantly weakened the binding of $RAP74_{436-517}$ to $FCP1_{879-961}$ (*45*). To test if the first leucine of the LXXLL-like motif within the central domain of FCP1 is required for $RAP74_{436-517}$ binding, we made a double alanine mutant (Y592A and L593A) version of $FCP1_{562-599}$ (Figure 6A). We observed significantly reduced binding of $RAP74_{436-517}$ to this double alanine mutant compared to its wild-type counterpart (Figure 6D). These results indicate that the central region of FCP1, like the carboxyl-terminal domain, binds to RAP74 through a small conserved acidic/hydrophobic motif. A summary of the in vitro binding results between RAP74 and GST-FCP1 fragments is presented in Figure 6E.

$FCP1_{579-600}$ Binds to a Shallow Groove between α Helices H2 and H3 on the Surface of the Carboxyl-Terminal Domain of RAP74. We have previously determined the NMR structure of the free carboxyl-terminal domain of RAP74 ($RAP74_{436-517}$) (*44*) and mapped the $FCP1_{879-961}$-binding domain on this structure by computing chemical-shift changes in $RAP74_{436-517}$ before and after formation of the $FCP1_{879-961}$/$RAP74_{436-517}$ complex (*44*). We found that $FCP1_{879-961}$ binds in a shallow groove formed by α helices H2 and H3 on the surface of RAP74 (*44*). Detailed views of the interaction were subsequently obtained from high-resolution structure determination of the $FCP1_{879-961}$/$RAP74_{436-517}$ complex by NMR spectroscopy (*45*) and of a similar complex by X-ray crystallography (*65*). Here we have also used chemical-shift mapping for studying the $FCP1_{579-600}$-binding site on this $RAP74_{436-517}$ domain (Figure 7A) (*66, 67*). The changes in amide resonance chemical shifts (Δ_{HN}) between the free $RAP74_{436-517}$ and the $FCP1_{579-600}$/$RAP74_{436-517}$ complex were calculated from 2D ^1H-^{15}N HSQC spectra (*55*) using the equation: $\Delta_{HN} = [(\Delta_H)^2 + (0.17 \times \Delta_N)^2]^{1/2}$. As observed previously with $FCP1_{879-961}$ (*44*), many of the amide resonances of RAP74 have similar chemical shifts between the free and bound forms of $RAP74_{436-517}$, indicating that the overall structure of RAP74 remains essentially the same in this complex. However, 33 out of the 82 amide resonances underwent significant chemical-shift changes ($\Delta \geq 0.13$ ppm), and these changes were mapped on the structure of free $RAP74_{436-517}$ (Figure 7B). Interestingly, the RAP74 residues affected by $FCP1_{579-600}$ binding are for the most part, the same as those affected by $FCP1_{879-961}$ binding (Figure 7B). It appears that, similarly to $FCP1_{879-961}$ (*44, 45*), $FCP1_{579-600}$ interacts with the shallow groove formed by α helices 2 and 3 on the carboxyl-terminal domain of RAP74.

Tat Blocks RAP74 Binding to FCP1 in Vitro. Our in vitro binding studies revealed that two regions of FCP1, the acidic/hydrophobic region and the BRCT domain, interact with Tat. Since the small acidic/hydrophobic motif, $FCP1_{579-600}$, that is essential for interaction with $RAP74_{436-517}$ lies within one of these regions, we were interested in determining if it was also involved in Tat-binding. GST-FCP1 fragments coupled to GSH-Sepharose resin were incubated with purified Tat_{1-86} in the absence or presence of $FCP1_{579-600}$ (Figure 8A). The

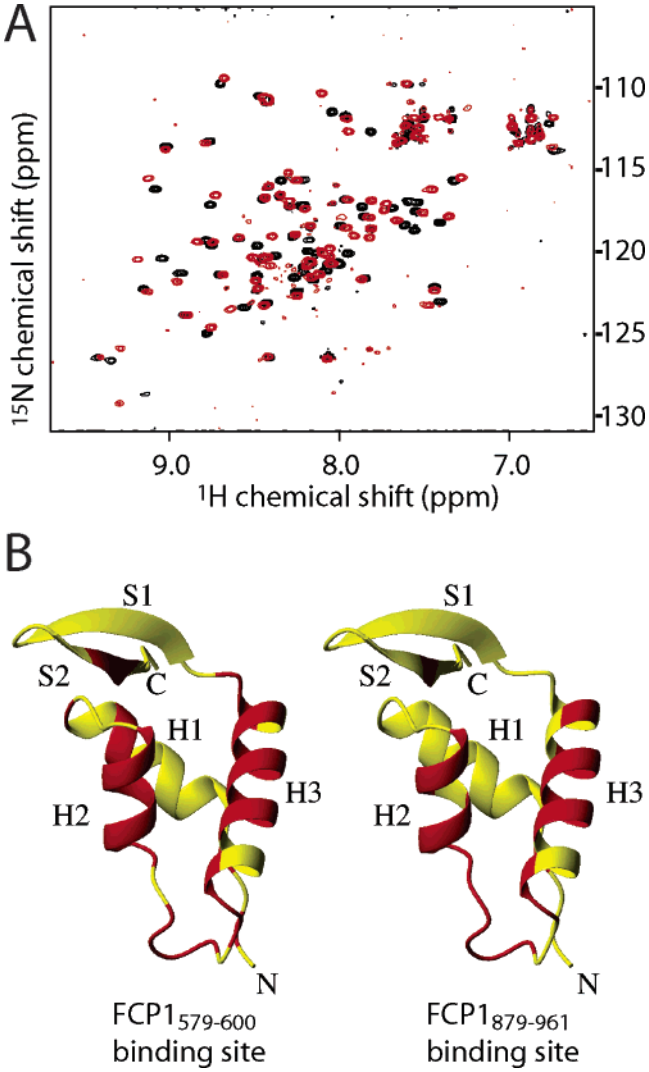

FIGURE 7: $FCP1_{579-600}$ binds to a shallow groove between α helices H2 and H3 on the surface of $RAP74_{436-517}$. (A) Overlay of 2D ^1H-^{15}N HSQC spectra of the free ^{15}N-labeled $RAP74_{436-517}$ (black) and of the ^{15}N-labeled $RAP74_{436-517}$/$FCP1_{579-600}$ complex (red). (B) Chemical-shift mapping of the $FCP1_{579-600}$-binding site (left) and $FCP1_{879-961}$-binding site (right) (*44*) on the ribbon diagram of $RAP74_{436-517}$. Residues for which we observed a significant change in amide chemical shifts {$\Delta_{HN} \geq 0.13$ ppm and $\Delta_{HN} = [(\Delta_H)^2 + (0.17 \times \Delta_N)^2]^{1/2}$} upon addition of $FCP1_{579-600}$ are indicated in red.

$FCP1_{579-600}$ peptide, which inhibits $RAP74_{436-517}$ binding to $FCP1_{562-619}$ (Figure 6C), did not inhibit Tat_{1-86} binding to either GST-$FCP1_{562-738}$ or GST-$FCP1_{562-619}$ even when the peptide concentration was 200 times higher than that of Tat_{1-86} (Figure 8A). Therefore, it appears that, unlike $RAP74_{436-517}$, Tat does not specifically recognize the small acidic/hydrophobic motif of $FCP1_{562-738}$. To verify these results, we tested if the binding of Tat_{1-86} to both GST-$FCP1_{562-738}$ and GST-$FCP1_{562-599}$ was affected by the double alanine substitution Y592A/L593A (Figure 8B). In vitro binding studies revealed that these mutant FCP1 fragments bound Tat_{1-86} as well as their wild-type counterparts, thereby confirming that the small hydrophobic motif is not essential for the Tat/FCP1 interaction (Figure 8B).

Because Tat recognizes sequences in FCP1 that extend on either sides of the RAP74-binding site, we were interested in determining if purified Tat could inhibit $RAP74_{436-517}$

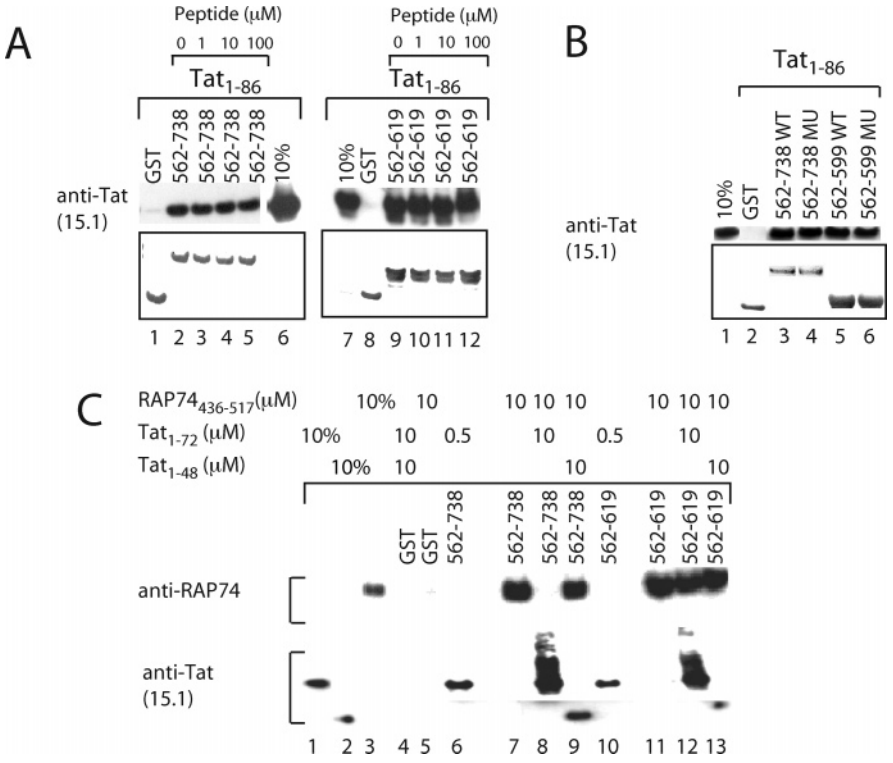

FIGURE 8: HIV-1 Tat inhibits $RAP74_{436-517}$ binding to the central domain of FCP1. (A) A small peptide derived from FCP1 ($FCP1_{579-600}$), which interacts with $RAP74_{436-517}$, does not inhibit the binding of Tat_{1-86} to the central domain of FCP1. GST-$FCP1_{562-738}$ (0.5 μM) or GST-$FCP1_{562-619}$ (2 μM) were incubated with purified Tat_{1-86} (0.5 μM) protein in the presence of increasing amounts of $FCP1_{579-600}$ (0, 1, 10 and 100 μM). (B) Alanine substitutions within the conserved hydrophobic motif do not affect Tat_{1-86} binding to the central domain of FCP1. We examined the interaction of Tat_{1-86} with the GST-$FCP1_{562-738}$ Y592A/L593A mutant (562−738 MU) and with the GST-$FCP1_{562-599}$ Y592A/L593A mutant (562−599 MU) as well as with the corresponding wild-type proteins (562−738 WT and 562−599 WT). Lane 1 shows 10% Tat_{1-86} input and lane 2 the control reaction with the GST protein. In lanes 2−4, each binding reaction contained 0.5 μM of Tat_{1-86} and 0.5 μM of GST or GST-fusion protein. In lanes 5 and 6, each binding reaction contained 0.5 μM of Tat_{1-86} and 2 μM of GST-fusion protein. (C) Tat_{1-72} inhibits $RAP74_{436-517}$ binding to FCP1, and the full BRCT domain is required for this inhibition. Purified $RAP74_{436-517}$, Tat_{1-72} or Tat_{1-48} proteins were added to binding reactions with 10 μM GST-$FCP1_{562-738}$ or GST-$FCP1_{562-619}$ as indicated (concentrations in μM). Lanes 1, 2, and 3 show 10% input of purified proteins and lanes 4 and 5 represent GST control reactions. For (A) and (B), bound Tat protein was detected using the Tat monoclonal antibody (15.1). For (C), bound $RAP74_{436-517}$ protein was detected using the RAP74 polyclonal antibody (C-18) and subsequently bound Tat_{1-48} and Tat_{1-72} were detected using the Tat monoclonal antibody (15.1). Figures (A)−(C) are shown as described in the legend of Figure 4.

binding to the central domain of FCP1 (Figure 8C). To do this, GST-$FCP1_{562-738}$ coupled to GSH-Sepharose resin was incubated with purified $RAP74_{436-517}$ in the absence or presence of purified HIV-1 Tat_{1-48} or Tat_{1-72}. At equimolar concentration, Tat_{1-72} completely inhibited $RAP74_{436-517}$ binding to GST-$FCP1_{562-738}$ (Figure 8C, lane 8), indicating that Tat_{1-72} has a higher affinity than $RAP74_{436-517}$ for GST-$FCP1_{562-738}$. However, under similar conditions Tat_{1-48} did not inhibit the interaction of $RAP74_{436-517}$ with GST-$FCP1_{562-738}$ (Figure 8C, lane 9), indicating that residues 48−86 of Tat are required for inhibition.

To evaluate if the BRCT domain was required for Tat to inhibit the binding of RAP74 to FCP1, we performed similar experiments as above but using a shorter FCP1 fragment, $FCP1_{562-619}$, which lacks the BRCT domain and is comprised of only a portion of the acidic/hydrophobic region (Figure 8C). When equimolar concentrations of Tat_{1-72} and $RAP74_{436-517}$ were allowed to bind GST-$FCP1_{562-619}$, both Tat_{1-72} and $RAP74_{436-517}$ interacted with FCP1 (Figure 8C, lane 12). Similar concentrations of Tat_{1-48} also did not prevent $RAP74_{436-517}$ binding to GST-$FCP1_{562-738}$ (Figure 8C, lane 13). These results indicate that the BRCT domain is required for Tat_{1-72} to inhibit the binding of $RAP74_{436-517}$ to the central domain of FCP1. This requirement for the BRCT domain presumably reflects the need for Tat_{1-72} to bind both the acidic/hydrophobic and BRCT domains of FCP1 in order to efficiently prevent $RAP74_{436-517}$ from interacting with this region.

Tat Inhibits CK2 Phosphorylation at a Novel Site within the Central Domain of FCP1. In the following paper in this issue, we describe the identification within the FCP1 acidic/hydrophobic region of a novel threonine CK2 phosphorylation site (T584 within the motif TDED), which is highly conserved among vertebrates (Figures 3 and 9A (*68*)). Interestingly, we found that phosphorylation of T584 by CK2 increases the binding of $FCP1_{562-619}$ to $RAP74_{436-517}$ (*68*). We were therefore interested in testing if phosphorylation of T584 by CK2 had any effect on Tat binding (Figure 9B). Binding reactions were set up using CK2-phosphorylated and nonphosphorylated GST-$FCP1_{562-619}$ with purified Tat_{1-86}. Although CK2 phosphorylation of GST-$FCP1_{562-619}$ enhances $RAP74_{436-517}$ binding (*68*), it did not affect Tat_{1-86} binding under the same conditions (Figure 9B, lanes 4 and 5). Furthermore, we found that a substitution of T584 by a glutamic acid (T584E) had little or no effect on interaction with Tat_{1-72}, and this regardless of whether the mutant protein was subjected or not to a CK2 phosphorylation reaction (Figure 9B, lanes 4 and 5). These results indicate that T584 does not contribute significantly to Tat binding.

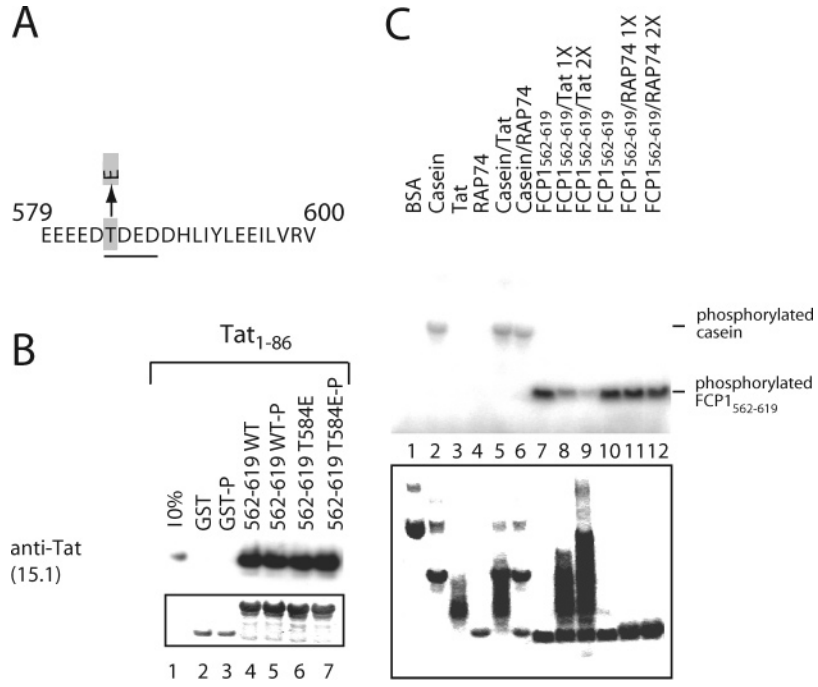

FIGURE 9: Role of a novel CK2 site within the acidic/hydrophobic region of the central domain of FCP1. (A) Sequence of $FCP1_{579-600}$ showing the location of the conserved CK2 site (TDED; underlined), the phosphorylated amino acid (T584; shaded) and the T584E mutation studied here. (B) Phosphorylation of T584 does not affect the binding of Tat_{1-86} to the central domain of FCP1. Lane 1 shows 10% Tat_{1-86} input and lanes 2 and 3 represent binding of Tat_{1-86} to the GST control resin after mock phosphorylation and phosphorylation reactions, respectively. Each binding reaction contained 0.5 μM of GST-$FCP1_{562-619}$ wild-type (562−619 WT) or GST-$FCP1_{562-619}$ mutant (562−619 T584E) and 0.5 μM Tat_{1-86}. Proteins were subjected to mock (GST, 562−619 WT or 562−619 T584E) or CK2 phosphorylation (GST-P, 562−619 WT-P or 562−619 T584E−P) reactions. Bound Tat_{1-86} was detected using the Tat monoclonal antibody (15.1). Figure (B) is shown as described in the legend of Figure 4. (C) The binding of Tat inhibits phosphorylation at T584 by CK2. Phosphorylation reactions were performed in the presence of [γ^{32}P]-ATP. Control phosphorylation reactions with BSA (lane 1), casein (lane 2), Tat_{1-86} (lane 3), RAP74 (lane 4), casein and Tat_{1-86} (lane 5) and casein and $RAP74_{436-517}$ (lane 6) are shown. CK2 phosphorylation of $FCP1_{562-619}$ (25 μg or 161 μM) in the absence (lane 7) or the presence of 1X (25 μg or 100 μM; lane 8) or 2X (50 μg or 200 μM; lane 9) Tat_{1-86}. CK2 phosphorylation of $FCP1_{562-619}$ (25 μg or 161 μM) in the absence (lane 10) or the presence of 1X (25 μg or 114 μM; lane 11) or 2X (50 μg or 228 μM; lane 12) $RAP74_{436-517}$. The ^{32}P-labeled proteins were detected by PhosphorImager analysis. A Coomassie blue stain of the gel (C) was performed to verify equivalent protein input (boxed).

Although the phosphorylation of T584 did not significantly affect Tat binding, we wanted to know if Tat binding could affect the phosphorylation level of T584. To answer this question, we tested if CK2 could phosphorylate FCP1 within a pre-assembled Tat_{1-86}/$FCP1_{562-619}$ complex (Figure 9C). We found that Tat inhibited CK2 phosphorylation of FCP1 in a concentration dependent manner (Figure 9C, lanes 7−9), but did not affect CK2 phosphorylation of the control casein sample (Figure 9C, lanes 2 and 5). By contrast, addition of $RAP74_{436-517}$ did not prevent CK2 phosphorylation of $FCP1_{562-619}$ (Figure 9C, lanes 10−12) and of the control casein sample (Figure 9C, lanes 2 and 6). Our results indicate that Tat not only prevents $RAP74_{436-517}$ binding to the central domain of FCP1, but also inhibits phosphorylation at a novel conserved CK2 site.

DISCUSSION

With this manuscript, we showed that FCP1 is essential for Tat-mediated transactivation of the HIV-1 LTR in vitro and that HIV-1 Tat and FCP1 directly interact both in the yeast two-hybrid system and in vitro. We then characterized in details the interactions of the central domain of FCP1 with Tat and the carboxyl-terminal domain of RAP74 (Figure 10) and investigated the role of CK2 phosphorylation on these interactions. These findings are discussed below in light of the potential functional implications of the FCP1/Tat interaction.

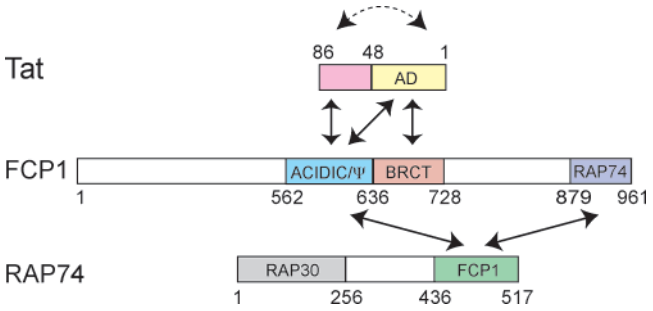

FIGURE 10: Summary of the interactions of FCP1 with HIV-1 Tat and RAP74. Arrows indicate interactions between highlighted domains. The dashed arrow illustrates the proposed interaction between the activation and carboxyl-terminal domains of Tat.

FCP1 Is Required for Tat-Activated Transcription in Vitro. The in vitro transcription results presented herein suggest that FCP1 is specifically required for Tat transactivation in vivo. Previous transfection studies indicated that FCP1 overexpression inhibits Tat-activated, but not Sp1-driven transcription (*69*). Although these two sets of results may appear contradictory, one can speculate that high concentrations of FCP1 in vivo have a dominant negative effect on Tat-activated transcription not observed in our in vitro studies. It is indeed possible that overexpression of FCP1 in vivo titrates out (squelch) the amount of Tat, RAP74 or other cellular factors necessary for Tat-mediated transactivation

of the HIV LTR. Hence, the results from these transfections studies do not really address if FCP1 is a positive or negative regulator of Tat transactivation. In contrast, our in vitro results with FCP1-depleted extracts, and their complementation by recombinant FCP1, clearly indicate that FCP1 is essential for Tat transactivation. As for the role of FCP1 in Sp1-driven basal transcription, both our in vitro studies and the in vivo transfection studies agree that FCP1 is not required. These last results suggest that FCP1 is not always required for transcription.

Tat Binds to Both the Acidic/Hydrophopic Region and the BRCT Domain of FCP1. Using our in vitro batch-affinity binding assay, we found that HIV-1 Tat interacts with two independent domains of FCP1, the amino-terminal portion of the acidic/hydrophobic region and the BRCT domain as summarized in Figure 10. In this assay, the binding of HIV-1 Tat (or Tat_{1-48}) to the central domain of FCP1 ($FCP1_{562-738}$) was comparable to that of Tat_{1-48} to the amino-terminal portion of the acidic/hydrophobic region ($FCP1_{562-619}$) or to the BRCT domain ($FCP1_{626-738}$). It is important to realize that our binding assay is not quantitative per se and may not always reveal small differences in binding affinity. Therefore, we cannot conclude at this moment on the relative affinity of Tat_{1-48} for the two subdomains of $FCP1_{562-738}$.

In general, we observed a good correlation between the results obtained with the batch-affinity binding assay in vitro and those obtained with the yeast two-hybrid system. In one case however, we noticed a difference between the results obtained with the in vitro binding assay and those obtained in yeast. Specifically, we observed reduced Tat binding in the yeast two-hybrid assay of the $FCP1_{562-637}$ fragment, whereas the comparable $FCP1_{562-619}$ fragment binds as well as the larger $FCP1_{562-738}$ in the batch-affinity binding assay. Further experiments will be needed to address if this discrepancy is significant. It may be that $FCP1_{562-619}$ has indeed a slightly weaker affinity for Tat, which was not revealed in our GST-pull down binding assay. Alternatively, the weaker signal observed in the two-hybrid assay may not be due to a weakened interaction but rather to other factors, such as a decrease in protein stability, impaired folding, mislocalization, etc.

Binding results with various Tat fragments, Tat_{1-72}, Tat_{1-48} and Tat_{48-86} are indicative of an antagonistic interplay between the activation domain and the carboxyl-terminal arginine-rich domain of Tat. Indeed, we found that Tat_{1-48} binds better than Tat_{1-72} to $FCP1_{626-738}$ and $FCP1_{599-738}$, and that Tat_{48-86} does not interact optimally with the acid-rich $FCP1_{562-599}$ in the context of the full-length Tat protein binding (Figure 4). These results are reminiscent of those observed with Tat-mediated transcriptional activation experiments, where the activation potential of Tat_{1-48} was greatly reduced in the context of longer Tat derivatives (*63*). In addition, a previous NMR study has shown that the amino-terminal portion of HIV-1 Tat (residues 4 to 11 and 32 to 47) forms a hydrophobic core that interacts with its glutamine-rich region (residues 60−76) (*62*). Intramolecular interactions between the activation domain and the carboxyl-terminal domain of Tat could explain the antagonist interplay between these two domains detected in our binding studies.

RAP74 Binds to the Acidic/Hydrophopic Region of FCP1. We characterized the interaction of FCP1 with RAP74 using an in vitro batch-affinity binding assay with purified proteins (Figure 10). We found that the carboxyl-terminal domain of RAP74 interacts with a small fragment of the acidic/hydrophobic region of FCP1, which contains a conserved LXXLL-like motif. This motif is similar to the one found in the carboxyl-terminal domain of FCP1 ($FCP1_{879-961}$) and involved in the $FCP1_{879-961}$/$RAP74_{436-517}$ interaction (*45*). We found that, like the H1′ α helix of $FCP1_{879-961}$, $FCP1_{579-600}$ interacts with the shallow groove formed by α helices H2 and H3 of the carboxyl-terminal domain of RAP74. Furthermore, secondary structure prediction of the $FCP1_{579-600}$ indicates that residues 593−600 within this fragment have a propensity to form an α helix (data not shown). $FCP1_{579-600}$ likely adopts an amphiphilic helix that forms hydrophobic interactions and key polar interactions with RAP74, as previously described for the $FCP1_{879-961}$/$RAP74_{436-517}$ complex (*45*). Residue T584, which is phosphorylated by CK2, is part of the minimal RAP74-binding domain identified here, $FCP1_{579-600}$, and is likely located at the interface of the $FCP1_{579-600}$/RAP74 complex (*68*). Favorable interactions between the phosphorylated T584 and RAP74 could explain the increased binding of $FCP1_{579-600}$ to RAP74 brought about by T584 phosphorylation. In this context, the reduced interaction of RAP74 with FCP1 when T584 is not phosphorylated would explain why RAP74 does not inhibit phosphorylation of $FCP1_{579-600}$. NMR structural studies are in progress to address the role of T584 in the $FCP1_{579-600}$/RAP74 interaction. It is interesting to note that the same domain of RAP74 interacts with both the central and the carboxyl-terminal domains of FCP1 (Figure 10). The functional significance of this observation is not yet understood. However, it has been previously shown that TFIIF forms an $\alpha_2\beta_2$ heterotetramer (*17, 70*), where two RAP74−RAP30 dimers assemble via homomeric RAP74 interactions (*70*). Formation of such a tetramer would be consistent with simultaneous binding of two RAP74 subunits to the two interacting domains of FCP1.

Tat Prevents the Interaction of RAP74 with FCP1. Our results indicate that both Tat and RAP74 bind to the acidic/hydrophobic region of FCP1 (Figure 10), but in different ways and in a mutually exclusive manner. Indeed we found that the HIV-1 Tat protein does not directly interact with the peptide fragment that contains the conserved acidic/hydrophobic motif and which is essential for the interaction with $RAP74_{436-517}$. Nevertheless, we have clearly shown that binding of the HIV-1 Tat protein to the central domain of FCP1 inhibits the binding of $RAP74_{436-517}$. The full-length HIV-1 Tat and the entire central domain of FCP1 are required for this inhibition. The inhibition of the RAP74/FCP1 interaction by Tat is intriguing in light of the fact that Tat and RAP74 do not appear to share a common binding site on the central domain of FCP1. It is possible that binding of Tat to FCP1 reduces the accessibility of the RAP74 binding site on FCP1, either by steric hindrance or as a result of a conformational change in the RAP74-binding site.

Similarity between the Acidic/Hydrophobic Region of FCP1 and the Inter-BRCT-Domain Linker of XRCC1. We have defined a conserved acidic/hydrophobic region adjacent to the BRCT domain, which is important for the Tat and RAP74 interactions with FCP1. In proteins with tandem BRCT repeats, the BRCT domains pack to form a compact structure, which involves an α helix from the linker region at the interface of the two repeats (*31, 33, 35*). The linker

between the BRCT domains often serves to stabilize the BRCT fold and may participate in ligand interactions (*24*). Interestingly, the conserved acidic/hydrophobic region of FCP1 has similarity to the acid-rich linker region located between the BRCT I and BRCT II domains of XRCC1, and, furthermore, there are two CK2 sites located in a conserved region of this linker (*71*). We propose that the conserved acidic/hydrophobic region in FCP1 similarly interacts with the BRCT domain and helps to strengthen its interaction with the Tat protein (see *Functional Implications of the FCP1/Tat Interaction* below). Given the importance of BRCT domains in protein−protein interactions, it is likely that BRCT domains form intramolecular interactions not only with adjacent BRCT domains, but with other protein domains as well. BRCT domains have been shown to be phosphopeptide recognition modules (*36*, *37*, *72*), therefore it is also likely that the strength of these intramolecular interactions could be controlled by phosphorylation. Further studies are needed to address the role of CK2 phosphorylation in promoting intramolecular interactions between the acidic/hydrophobic region and the BRCT domain of FCP1.

Functional Implications of the FCP1/Tat Interaction. Although Tat inhibits the phosphatase activity of FCP1 (*40*), and FCP1 is essential for in vitro transcriptional transactivation by Tat (this study), the molecular details of these functional interactions have remained unclear. Our binding studies were aimed at elucidating some of these interactions. We suspect that the direct binding between HIV-1 Tat and FCP1 that we have characterized in this study is essential for Tat to inhibit the CTD phosphatase activity of FCP1 and to promote transactivation of the HIV LTR. In support of this, we found that the C22G mutation in Tat that impairs its transactivation potential also affects its interaction with FCP1.

We have shown that Tat prevents the interaction of RAP74 with FCP1, suggesting that one mechanism by which Tat inhibits the phosphatase activity is by preventing RAP74 from interacting with FCP1 and from stimulating its enzymatic activity. This may be only one mode of phosphatase inhibition by Tat, since it has been shown that Tat inhibits the CTD phosphatase activity of FCP1 in the absence of RAP74 (*40*). Tat may also block amino acids or posttranslational modifications that are essential for the phosphatase activity of FCP1 or induce a conformational change in FCP1 that inhibits its phosphatase activity. Indeed, previous reports suggest that the Tat-binding domain of FCP1 is essential for phosphatase activity (*9*, *38*). Studies performed with human FCP1 have demonstrated that free RNAPIIO can be dephosphorylated by a FCP1 mutant which lacks the carboxyl-terminal RAP74 binding domain, however further deletions of the central Tat-binding domain was detrimental for activity (*9*). In addition, a recent deletion analysis of *S. pombe* FCP1 reveals that the minimal contiguous sequence necessary for phosphatase activity includes the FCP1 homology domain at the amino terminus and the BRCT domain at the carboxyl terminus (*38*).

It has been previously demonstrated that Tat inhibits the FCP1 phosphatase activity and prevents CTD dephosphorylation of early elongation complex initiated from the HIV-1 LTR template (*40*, *73*). These results are consistent with the idea that Tat inhibition of CTD phosphatase activity plays a role in transcriptional activation by Tat (*73*). However, the role of FCP1 in transcriptional elongation was also shown to be independent of its phosphatase activity (*9*, *15*), pointing toward the phosphatase activity being dispensable for the effect of Tat on transcriptional elongation. Furthermore, we showed here that addition of FCP1 to an FCP1-depleted extract activates Tat-dependent transcription, indicating that Tat transactivation does not only result from inhibition of an existing phosphatase activity. Clearly, activities other than the phosphatase activity are essential for transactivation by HIV-1 Tat.

To exert its transactivation effect Tat may require FCP1 for its role as a positive elongation factor. Tat may simply help recruit FCP1 or stabilize the interaction of FCP1 to the early elongation complex. Although FCP1 functions in elongation complexes (*9*, *14*, *15*), a stable stoichiometric association with RNAPIIO has not been demonstrated (*11*, *16*) and factors may be required to recruit FCP1 to elongating complexes. It is also possible that the interaction of Tat with FCP1 prevents negative transcription elongation factors from interacting with FCP1 and/or the elongating transcription complex. Similarly, it has been previously demonstrated that the positive transcription elongation effects of TFIIF are partly due to competition with the negative elongation factor NELF (*74*). Another interesting possibility is that FCP1 serves as a molecular switch, and when Tat interacts with FCP1 a conformational change occurs within FCP1 and/or the transcription complex that enhances transcriptional elongation. Our results suggest that an intramolecular interaction between the acidic/hydrophobic region and the BRCT domain prevent optimal binding of Tat_{48-86}. Although further studies are necessary to confirm this intramolecular interaction in the central domain of FCP1, it may have important implications for the regulation of FCP1 functions.

Tat Inhibits the Phosphorylation of FCP1 by CK2. In the following paper in this issue, we report on the identification of a novel CK2 phosphorylation site (T584) located within the Tat-binding domain of FCP1 (*68*). In this study, we found that Tat is able to inhibit phosphorylation by CK2 at this site. This phosphorylation event may therefore be an additional important regulator of the phosphatase activity and/or the positive transcription elongation effect of FCP1. Indeed, it was recently established that phosphorylation of *X. Laevis* FCP1 by CK2 enhances the phosphatase activity of FCP1 and binding to RAP74 (*42*). We therefore propose that one mechanism by which Tat inhibits FCP1 phosphatase activity is by blocking CK2 phosphorylation of FCP1, which could affect the phosphatase activity directly or indirectly by preventing RAP74 binding to the central domain of FCP1 (*68*). Alternatively, it was recently found that CK2 inhibits the positive transcription elongation effect of FCP1 (*43*). In this view, Tat could also function by preventing the CK2 inhibition and thereby promoting the positive transcription elongation effect of FCP1. Finally, phosphorylation of FCP1 by CK2 may serve to regulate a function not yet defined for FCP1 that is regulated by Tat. Further studies will be required to test these different possibilities and also to investigate if this particular CK2 site is involved in Tat-mediated transactivation in vivo. It also remains to be shown if other posttranslational modifications of FCP1 affects its roles as a phosphatase, as a positive elongation factor and as a mediator of Tat transactivation.

ACKNOWLEDGMENT

We thank the NIH AIDS Research and Reference Reagent Program for HIV-1 Tat expression vectors and antibodies, Q. Zhou and P.A. Sharp for the pHIV+TAR-G400 template, M. Dahmus for full-length FCP1 Mono Q fraction 34, Danny Reinberg for providing the full-length hFCP1 clone, Barbara Potempa for assistance in the preparation of protein samples and Claiborne Glover for critical reading of the manuscript.

REFERENCES

1. Payne, J. M., Laybourn, P. J., and Dahmus, M. E. (1989) The transition of RNA polymerase II from initiation to elongation is associated with phosphorylation of the carboxyl-terminal domain of subunit IIa, *J. Biol. Chem. 264*, 19621−19629.
2. Weeks, J. R., Hardin, S. E., Shen, J., Lee, J. M. and Greenleaf, A. L. (1993) Locus-specific variation in phosphorylation state of RNA polymerase II *in vivo*: Correlations with gene activity and transcript processing, *Genes Dev. 7*, 2329−2344.
3. Corden, J. L. (1990) Tails of RNA polymerase II, *Trends Biochem. Sci. 15*, 383−387.
4. Marshall, N. F., Peng, J., Xie, Z., and Price, D. H. (1996) Control of RNA polymerase II elongation potential by a novel carboxyl-terminal domain kinase, *J. Biol. Chem. 271*, 27176−27183.
5. Lu, H., Zawel, L., Fisher, L., Egly, J. M., and Reinberg, D. (1992) Human general transcription factor IIH phosphorylates the C-terminal domain of RNA polymerase II, *Nature 358*, 641−645.
6. Kobor, M. S., and Greenblatt, J. (2002) Regulation of transcription elongation by phosphorylation, *Biochim. Biophys. Acta 1577*, 261−275.
7. Chambers, R. S., and Dahmus, M. E. (1994) Purification and characterization of a phosphatase from HeLa cells which dephosphorylates the C-terminal domain of RNA polymerase II, *J. Biol. Chem. 269*, 26243−26248.
8. Archambault, J., Pan, G., Dahmus, G. K., Cartier, M., Marshall, N., Zhang, S., Dahmus, M. E., and Greenblatt, J. (1998) FCP1, the RAP74-interacting subunit of a human protein phosphatase that dephosphorylates the carboxy-terminal domain of RNA polymerase IIO, *J. Biol. Chem. 273*, 27593−27601.
9. Cho, H., Kim, T. K., Mancebo, H., Lane, W. S., Flores, O., and Reinberg, D. (1999) A protein phosphatase functions to recycle RNA polymerase II, *Genes Dev. 13*, 1540−1552.
10. Schroeder, S. C., Schwer, B., Shuman, S., and Bentley, D. (2000) Dynamic association of capping enzymes with transcribing RNA polymerase II, *Genes Dev. 14*, 2435−2440.
11. Cho, E.-J., Kobor, M. S., Kim, M., Greenblatt, J., and Buratowski, S. (2001) Opposing effects of Ctk1 kinase and Fcp1 phosphatase at Ser 2 of the RNA polymerase II C-terminal domain, *Genes Dev. 15*, 3319−3329.
12. Hausmann, S., and Shuman, S. (2002) Characterization of the CTD phosphatase Fcp1 from fission yeast. Preferential dephosphorylation of serine 2 versus serine 5, *J. Biol. Chem. 277*, 21213−21220.
13. Lin, P. S., Dubois, M.-F., Dahmus, M. E. (2002) TFIIF-associating carboxyl-terminal domain phosphatase dephosphorylates phosphoserines 2 and 5 of RNA polymerase II, *J. Biol. Chem. 277*, 45949−45956.
14. Lehman, A. L., and Dahmus, M. E. (2000) The sensitivity of RNA polymerase II in elongation complexes to C-terminal domain phosphatase, *J. Biol. Chem. 275*, 14923−14932.
15. Mandal, S. S., Cho, H., Kim, S., Cabane, K., and Reinberg, D. (2002) FCP1, a phosphatase specific for the heptapeptide repeat of the largest subunit of RNA polymerase II, stimulates transcription elongation, *Mol. Cell. Biol. 22*, 7543−7552.
16. Kimura, M., Suzuki, H., and Ishihama, A. (2002) Formation of a carboxy-terminal domain phosphatase (Fcp1)/TFIIF/RNA polymerase II (pol II) complex in *Schizosaccharomyces pombe* involves direct interaction between Fcp1 and the Rpb4 subunit of pol II, *Mol. Cell. Biol. 22*, 1577−1588.
17. Jeronimo, C., Langelier, M.-F., Zeghouf, M., Cojocaru, M., Bergeron, D., Baali, D., Forget, D., Mnainmneh, S., Davierwala, A. P., Pootoolal, J., Chandy, M., Canadien, V., Beattie, B. K., Richards, D. P., Workman, J. L., Hughes, T. R., Greenblatt, J., and Coulombe, B. (2004) RPAP1, a novel human RNA polymerase II-associated protein affinity purified with recombinant wild-type and mutated polymerase subunits, *Mol. Cell. Biol. 24*, 7043−7058.
18. Archambault, J., Chambers, R. S., Kobor, M. S., Ho, Y., Cartier, M., Bolotin, D., Andrews, B., Kane, C. M., and Greenblatt, J. (1997) An essential component of a C-terminal domain phosphatase that interacts with transcription factor IIF in *Saccharomyces cerevisiae*, *Proc. Natl. Acad. Sci. U.S.A. 94*, 14300−14305.
19. Kobor, M. S., Archambault, J., Lester, W., Holstege, F. C. P., Gileadi, O., Jansma, D. B., Jennings, E. G., Kouyoumdjian, F., Davidson, A. R., Young, R. A., and Greenblatt, J. (1999) An unusual eukaryotic protein phosphatase required for transcription by RNA polymerase II and CTD dephosphorylation in *S. cerevisiae*, *Mol. Cell 4*, 55−62.
20. Collet, J. F., Stroobant, V., Pirard, M., Delpierre, G., and Schaftingen, E. V. (1998) A new class of phosphotransferases phosphorylated on an aspartate residue in an amino-terminal DXDX(T/V) motif, *J. Biol. Chem. 273*, 14107−14112.
21. Kobor, M. S., Simon, L. D., Omichinski, J., Zhong, G., Archambault, J., and Greenblatt, J. (2000) A motif shared by TFIIF and TFIIB mediates their interaction with the RNA polymerase II carboxy-terminal domain phosphatase Fcp1p in *Saccharomyces cerevisiae*, *Mol. Cell. Biol. 20*, 7438−7449.
22. Gaboriaud, C., Bissery, V., Benchetrit, T., and Mornon, J. P. (1987) Hydrophobic cluster analysis: an efficient new way to compare and analyze amino acid sequences, *FEBS Lett. 224*, 149−155.
23. Bork, P., Hofmann, K., Bucher, P., Neuwald, A. F., Altschul, S., and Koonin, E. V. (1997) A superfamily of conserved domains in DNA damage-responsive cell cycle checkpoint proteins, *FASEB J 11*, 68−76.
24. Callebaut, I., and Mornon, J.-P. (1997) From BRCA1 to RAP1: a widespread BRCT module closely associated with DNA repair, *FEBS Lett. 400*, 25−30.
25. Taylor, R. M., Thistlethwaite, A., and Caldecott, K. W. (2002) Central role for the XRCC1 BRCT I domain in mammalian DNA single-strand break repair, *Mol. Cell. Biol. 22*, 2556−2563.
26. Morales, J. C., Xia, Z., Lu, T., Aldrich, M. B., Wang, B., Rosales, C., Kellems, R. E., Hittelman, W. N., Elledge, S. J., and Carpenter, P. B. (2003) Role for the BRCA1 C-terminal repeats (BRCT) protein 53BP1 in maintaining genomic stability, *J. Biol. Chem. 278*, 14971−14977.
27. Miyake, T., Hu, Y.-F., Yu, D. S., and Li, R. (2000) A functional comparison of BRCA1 C-terminal domains in transcription activation and chromatin remodeling, *J. Biol. Chem. 275*, 40169−40173.
28. Ye, Q., Hu, Y.-F., Zhong, H., Nye, A. C., Belmont, A. S., and Li, R. (2001) BRCA1-induced large-scale chromatin unfolding and allele-specific effects of cancer-predisposing mutations, *J. Cell Biol. 155*, 911−921.
29. Zhang, Z., Morera, S., Bates, P. A., Whitehead, P. C., Coffer, A. I., Hainbucher, K., Nash, R. A., Sternberg, M. J. E., Lindahl, T., and Freemont, P. S. (1998) Structure of an XRCC1 BRCT domain: a new protein:protein interaction module, *EMBO J. 17*, 6404−6411.
30. Lee, J. Y., Chang, C., Song, H. K., Moon, J., Yang, J. K., Kim, H.-K., Kwon, S.-T., and Suh, S. W. (2000) Crystal structure of NAD+-dependent DNA ligase: modular architecture and functional implications, *EMBO J. 19*, 1119−1129.
31. Joo, W. S., Jeffrey, P. D., Cantor, S. B., Finnin, M. S., Livingston, D. M., and Pavletich, N. P. (2002) Structure of the 53BP1 BRCT region bound to p53 and its comparison to the Brca1 BRCT structure, *Genes Dev. 16*, 583−593.
32. Krishnan, V. V., Thornton, K. H., Thelen, M. P., and Cosman, M. (2001) Solution structure and backbone dynamics of the human DNA ligase IIIa BRCT domain, *Biochemistry 40*, 13158−13166.
33. Williams, R. S., Green, R., and Glover, J. N. M. (2001) Crystal structure of the BRCT repeat region from the breast cancer-associated protein BRCA1, *Nature Struct. Biol. 8*, 838−842.
34. Williams, R. S., and Glover, J. N. M. (2003) Structural consequences of a cancer-causing BRCA1-BRCT missense mutation, *J. Biol. Chem. 278*, 2630−2635.
35. Derbyshire, D. J., Basu, B. P., Serpell, L. C., Joo, W. S., Date, T., Iwabuchi, K., and Doherty, A. J. (2002) Crystal structure of human 53BP1 BRCT domains bound to p53 tumour suppressor, *EMBO J. 21*, 3863−3872.
36. Yu, X., Chini, C. C. S., He, M., Mer, G., and Chen, J. (2003) The BRCT domain is a phospho-protein binding domain, *Science*, 639−642.

37. Manke, I. A., Lowery, D. M., Nguyen, A., and Yaffe, M. B. (2003) BRCT repeats as phosphopeptide-binding modules involved in protein targetting, *Science 302*, 636−639.
38. Hausmann, S., and Shuman, S. (2003) Defining the active site of *Schizosaccharomyces pombe* C-terminal domain phosphatase Fcp1, *J. Biol. Chem. 278*, 13627−13632.
39. Chambers, R. S., Wang, B. Q., Burton, Z. F., and Dahmus, M. E. (1995) The activity of COOH-terminal domain phosphatase is regulated by a docking site on RNA polymerase II and by the general transcription factors IIF and IIB, *J. Biol. Chem. 270*, 14962−14969.
40. Marshall, N. F., Dahmus, G. K., and Dahmus, M. E. (1998) Regulation of carboxyl-terminal domain phosphatase by HIV-1 Tat protein, *J. Biol. Chem. 273*, 31726−31730.
41. Zhou, M., Halanski, M. A., Radonovich, M. F., Kashanchi, F., Peng, J., Price, D. H., and Brady, J. N. (2000) Tat modifies the activity of CDK9 to phosphorylate serine 5 of the RNA polymerase II carboxyl-terminal domain during human immunodeficiency virus type I transcription, *Mol. Cell. Biol. 20*, 5077−5086.
42. Palancade, B., Dubois, M.-F., and Bensaude, O. (2002) FCP1 phosphorylation by casein kinase 2 enhances binding to TFIIF and RNA polymerase II carboxyl-terminal domain phosphatase activity, *J. Biol. Chem. 277*, 36061−36067.
43. Friedl, E. M., Lane, W. S., Erdjument-Bromage, H., Tempst, P., and Reinberg, D. (2003) The C-terminal domain phosphatase and transcription elongation activities of FCP1 are regulated by phosphorylation, *Proc. Natl. Acad. Sci. U.S.A. 100*, 2328−2333.
44. Nguyen, B. D., Chen, H.-T., Kobor, M. S., Greenblatt, J., Legault, P., and Omichinski, J. G. (2003) Solution structure of the carboxyl-terminal domain of RAP74 and NMR characterization of the FCP1-binding sites of RAP74 and human TFIIB, *Biochemistry 42*, 1460−1469.
45. Nguyen, B. D., Abbott, K. L., Potempa, K., Kobor, M. S., Archambault, J., Greenblatt, J., Legault, P., and Omichinski, J. G. (2003) NMR structure of a complex containing the TFIIF subunit RAP74 and the RNA polymerase II carboxyl-terminal domain phosphatase FCP1, *Proc. Natl. Acad. Sci. U.S.A. 100*, 5688−5693.
46. Campioni, D., Corallini, A., Zauli, G., Possati, L., Altavilla, G., and Barbanti-Brodano, G. (1995) HIV type 1 extracellular Tat protein stimulates growth and protects cells of BK virus/tat transgenic mice from apoptosis, *Retroviruses 11*, 1039−1048.
47. Hauber, J., Perkins, A., Heiner, E., and Cullen, B. (1987) Transactivation of human immunodeficiency virus gene expression is mediated by nuclear events, *Proc. Natl. Acad. Sci. U.S.A. 84*, 6364−6368.
48. Rhim, H., Echetebu, C. O., and Rice, A. P. (1994) Wild type and mutant HIV-1 and HIV-1 Tat proteins expressed in *E. coli* as fusions with glutathione S-transferase, *J. Acquired Immune Defic. Syndr. 7*, 1116−1121.
49. Zhou, Q., and Sharp, P. A. (1995) Novel mechanism and factor for regulation by HIV-1 Tat, *EMBO J. 14*, 321−328.
50. Dignam, J. D., Lebovitz, R. M., and Roeder, R. G. (1983) Accurate transcription initiation by RNA polymerase II in a soluble extract from isolated mammalian nuclei, *Nucleic Acids Res. 11*, 1475−1489.
51. Ge, H., and Roeder, R. G. (1994) The high mobility group protein HMG1 can reversibly inhibit class II gene transcription by interaction with the TATA-binding protein, *J. Biol. Chem. 269*, 17136−17140.
52. Lapsia, M. F., Rice, A. P., and Mathews, M. B. (1989) HIV-1 Tat protein increases transcriptional initiation and stabilizes elongation, *Cell 59*, 283−292.
53. Sherman, F., Fink, G. R., and Hicks, J. B. (1986) *Laboratory course manual for methods in yeast genetics*, Cold Spring Harbor Laboratory Press, Cold Spring Harbor, N. Y.
54. Pace, C. N., Vajdos, F., Fee, L., Grimsley, G., and Gray, T. (1995) How to measure and predict the molar absorption coefficient of a protein, *Protein Science 4*, 2411−2423.
55. Kay, L. E., Keifer, P., and Saarinen, T. (1992) Pure absorption gradient enhanced heteronuclear single quantum correlation spectroscopy with improved sensitivity, *J. Am. Chem. Soc. 114*, 10663−10665.
56. Delaglio, F., Grzesiek, S., Vuister, G. W., Zhu, G., Pfeifer, J., and Bax, A. (1995) NMRPipe: a multidimensional spectral processing system based on UNIX pipes, *J. Biomol. NMR 6*, 277−293.
57. Southgate, C. D., and Green, M. R. (1991) The HIV-1 Tat protein activates transcription from an upstream DNA-binding site: implications for Tat function, *Genes Dev. 5*, 2496−2507.
58. Blau, J., Xiao, H., MacCracken, S., O'Hare, P., Greenblatt, J., and Bently, D. (1996) Three functional classes of transcriptional activation domain, *Mol. Cell Biol. 16*, 2044−2055.
59. Sonnhammer, E. L. L., Eddy, S. R., and Durbin, R. (1997) Pfam: a comprehensive database of protein domain families based on seed alignments, *Proteins 28*, 405−420.
60. Altschul, S. F., Madden, T. L., Schaffer, A. A., Zhang, J., Zhang, Z., Miller, W., and Lipman, D. J. (1997) Gapped BLAST and PSI−BLAST: a new generation of protein database search programs, *Nucleic Acids Res. 25*, 3389−3402.
61. Kato, H., Sumimoto, H., Pognonec, P., Chen, C.-H., Rosen, C. A., and Roeder, R. G. (1992) HIV-1 Tat acts as processivity factor *in vitro* in conjunction with cellular elongation factors, *Genes Dev. 6*, 655−666.
62. Bayer, P., Kraft, M., Ejchart, A., Westendorp, M., Frank, R., and Rosch, P. (1995) Structural studies of HIV-1 Tat protein, *J. Mol. Biol. 247*, 529−535.
63. Subramanian, T., D'Sa-Eipper, C., Elangovan, B., and Chinnadurai, G. (1994) The activation region of the Tat protein of human immunodeficiency virus type-1 functions in yeast, *Nucleic Acids Res 22*, 1496−1499.
64. Baldi, P., Brunak, S., Frasconi, P., Soda, G., and Pollastri, G. (1999) Exploiting the past and the future in protein secondary structure prediction, *Bioinformatics 15*, 937−946.
65. Kamada, K., Roeder, R. G., and Burley, S. K. (2003) Molecular mechanism of recruitment of TFIIF-associating RNA polymerase C-terminal domain phosphatase (FCP1) by transcription factor IIF, *Proc. Natl. Acad. Sci. U.S.A. 100*, 2296−2299.
66. Farmer, B. T., Constantine, K. L., Goldfarb, V., Friedrichs, M. S., Wittekind, M., Yanchunas, J., Robertson, J. G., and Mueller, L. (1996) Localizing the NADP+ binding site on the MurB enzyme by NMR, *Nature Struct. Biol. 3*, 995−997.
67. Shuker, S. B., Hajduk, P. J., Meadows, R. P., and Fesik, S. W. (1996) Discovering high-affinity ligands for proteins: SAR by NMR, *Science 274*, 1531−1534.
68. Abbott, K. L., Renfrow, M. B., Chalmers, M. J., Nguyen, B. D., Marshall, A. G., Legault, P., and Omichinski, J. G. (2004) Enhanced Binding of RNAPII CTD Phosphatase FCP1 to RAP74 following CK2 Phosphorylation, *Biochemistry 44*, 2732−2745.
69. Licciardo, P., Napolitano, G., Majello, B., and Lania, L. (2001) Inhibition of Tat transactivation by the RNA polymerase II CTD-phosphatase FCP1, *AIDS 15*, 301−307.
70. Robert, F., Douziech, M., Forget, D., Egly, J.-M., Greenblatt, J., Burton, Z. F., and Coulombe, B. (1998) Wrapping of the promoter DNA around the RNA polymerase II initiation complex induced by TFIIF, *Mol. Cell 2*, 341−351.
71. Marintchev, A., Robertson, A., Dimitriadis, E. K., Prasad, R., Wilson, S. H., and Mullen, G. P. (2000) Domain specific interaction in the XRCC1-DNA polymerase b complex, *Nucleic Acids Res. 28*, 2049−2059.
72. Caldecott, K. W. (2003) The BRCT domain: signaling with friends?, *Science 302*, 579−580.
73. Marshall, N. F., and Dahmus, M. E. (2000) C-terminal domain phosphatase sensitivity of RNA polymerase II in early elongation complexes on the HIV-1 and adenovirus 2 major late templates, *J. Biol. Chem. 275*, 32430−32437.
74. Renner, D. B., Yamaguchi, Y., Wada, T., and Price, D. H. (2001) A highly purified RNA polymerase II elongation control system, *J. Biol. Chem. 276*, 42601−42609.

BI047957P